Haukur Ingason
Sören Gustavsson
Martin Dahlberg

Heat Release Rate Measurements in Tunnel Fires

BRANDFORSK project 723-924

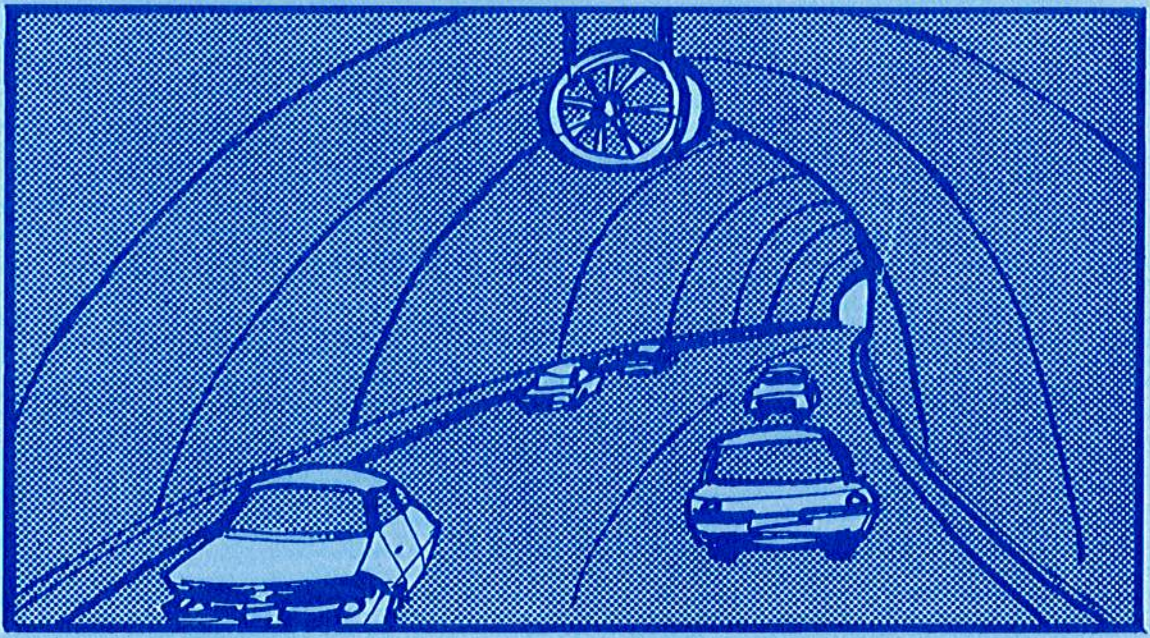

SP
Swedish National Testing and Research Institute
Fire Technology
SP REPORT 1994:08

Abstract

This report describes measurements of heat release rates in tunnel fires by using the oxygen consumption technique. This technique is commonly used in fire laboratories to measure heat release rates up to 10 MW. Measured heat release rates from fire tests with vehicles (a train, a bus, a subway coach and a simulated truck load) and wood cribs are presented.

The total heat release rate was determined by measuring oxygen concentrations and mass flow rates over the tunnel cross section at both sides of the fire. The convective fraction of the heat release rate was determined by measuring the temperature and the mass flow rate.

The technique is found to work reasonably well for tunnel fires. However, the measured convective fraction of the heat release rate need to be corrected for heat losses from the hot ceiling jet to the cold walls. The total heat release rate need to be corrected for high yields of carbon monoxide (CO_2) in the exhaust gases and for vitiation of the inflowing air in the lower part of the cross section.

The study is a joint project between a number of European countries with a project name EUREKA EU 499 Firetun.

Key words: heat release rate, tunnel, calorimetry, oxygen consumption

SP
SP Rapport 1994:08
ISBN 91-7848-XXX-X
Borås 1994

Swedish National Testing and Research Institute
SP REPORT 1994:08

Postal address:
Box 857, S-501 15 BORÅS, Sweden
Telephone + 46 33 16 50 00
Telex 36252 Testing S
Telefax + 46 33 13 55 02

Table of contents

Table of contents (cont) **page**

1 Summary

SP-Fire Technology was one of a number of European organisations which participated in a project named EUREKA EN 499 "Fires in Tunnels", a co-operation project where the main objective was to form a sound engineering basis for future design of road and railway tunnels [1]. Fire tests were carried out in a 2.3 km long abandoned mining tunnel in Norway to measure smoke generation, transient flow fields, optical densities, gas concentrations and heat release rates from burning vehicles. SP measured the heat release rates in 6 of totally 20 fire tests and the data is presented in this report.

Knowledge about the heat release rate is essential in fire engineering design of tunnels. Already a number of complex construction works have been designed with support of powerful computer CFD codes (Computational Fluid Dynamics). Such fire simulations are highly dependent on the accuracy of the design fire, i.e. the assumed heat release rate of the burning object. Therefore it was considered important to obtain such information in the test series with as good accuracy as possible. The results from tests with burning vehicles (a train, a bus, a subway coach, a simulated truck load) and two wood crib tests are presented here.

The heat release rates were determined with aid of two different methods. Firstly, by measuring the temperature, and mass flow rate and thus getting the convective fraction of the heat release rate and secondly, by measuring the oxygen (O_2) concentration and mass flow rate and thus getting the total heat release rate. For open hydrocarbon fires the convective fraction is rarely less than 60 to 70 percent of the total heat release rate [2]. The convective energy is carried away by the plume above the flames, while the remainder of the total heat released is radiated away. However, the experimental results show that the convective fraction is only 30 to 40 percent of the total heat release rate. This difference can be explained by heat losses from the hot ceiling jet to the cold walls between the fire source and the measurement stations.

There are a number of problems related to the use of oxygen consumption technique in tunnels which need to be discussed. The vertical variation of temperature, velocity and gas concentration is usually great in stratified counter flow as in tunnels with natural ventilation. Thus, the method requires many measuring probes to obtain reliable data for the heat release rate calculations. An estimation of the maximum error of the total heat release rate data is found to be in the order of ±25 % (relative errors conservatively added) and for comparison, the maximum error of the SP Industry Calorimeter [3], which is used in the laboratory to measure fires up to a 10 MW, is estimated to be less than ± 16%. To improve the method for tunnel application a more extensive instrumentation is required, especially the number of gas probes (O_2, CO_2) has to be increased. Only three probes were used on each side in the present experiments located in the upper part of the cross section. Based on experience with this technique at least three probes should be mounted in the lower part of the cross section as well. Furthermore, asymmetrically placed probes used to check the horizontal distribution are necessary.

Another problem with the technique is that the hot fire gases in the upper part will gradually cool and the smoke layer will descend to the floor level further away from the fire and mix with the incoming air. Thus, there will be a gradual re-entrainment of fire gases and consequently, due to lower oxygen concentrations and higher temperatures than otherwise in the incoming air, the calculated heat release rates will be overestimated if this is not taken into consideration. Thus the O_2 and the CO_2 concentrations must be measured both in the exhausted and the incoming gases. There is also an uncertainty in the horizontal concentration

distribution (assumed constant in the calculations) along with the uncertainty in the position of the oxygen concentration neutral layer. A knowledge about the location of the neutral layer for temperature, velocity and gas concentrations is very important for the method used here.

Similar principles for calculating the heat release rate are used in many fire laboratories [3,4,5]. The hot gases from the fire are collected to a duct system where all necessary analysis is carried out in one instrument station. The instrument station is located where the flow is well mixed and the measurements are made with only a small number of probes (usually one for temperature and velocity and a sampling probe for measurement of gas concentration). However, in the tunnel situation a different method is required to be able to integrate the mass flow rates (temperature and velocity) and the gas concentrations (O_2, CO_2 and CO) in the varying flow field across the cross section. A use of a sampling probe as in a duct system for measuring gas concentration is not possible in tunnels with natural ventilation, since the flow is usually bi-directional over the cross-section.

2 Background to the tests

The experiments presented here are included in a test programme worked out by EUREKA 499 (EU499); Fires in Tunnels. EUREKA was formed in 1985 to promote collaboration in high technology projects in Europe. EUREKA consists of 20 European member countries where the main objective is to avoid duplication of work, share costs, transfer technology, share risks and to promote business opportunities between these countries. The EUREKA project EU499 was announced in 1990 where Austria, Switzerland, Germany, France, Italy, Sweden, Norway, UK and Finland showed greatest interest in the project. Sweden was particularly interested in quantifying the heat energy produced by different types of burning vehicles.

The EU499 project was originally divided into 4 major areas; fire-fighting, communications, escape and rescue. The research programme was aimed to highlight in particular the following aspects:

- determination of transient rates of heat release, production of toxic gases and smoke, and change in visibility

- function of fire alarms, effectiveness of emergency lighting and escapeway systems

- heat transfer from convective ceiling flow to the walls

- obtain information for future verification of advanced computer models

- outline the toxic environment in tunnel fires

Successful computer simulations of fires in large complicated construction works like road and railway tunnels are highly dependent on the accuracy of the input data. The most important input parameter is the heat release rate from the burning objects. Research workers throughout the world have tried to effectively measure heat release rates from burning materials for many years. In tunnels this have, traditionally, been done by weighing the burning objects. This method can, however, be ambiguous due to the heavy weight of the tested vehicles.

The utilisation of oxygen consumption calorimetry has become the dominant method in determining heat release rate in fire laboratories today. Oxygen consumption calorimetry is based on the fact that for most materials a constant net amount of heat is released per unit mass of oxygen consumed in the combustion, 13.1 MJ/g O_2 [6,7,8]. Thus heat release rates can be readily measured if all combustion products from an experiment are collected in an extraction system and the flow and oxygen concentration in that duct is accurately measured. As a standard procedure corrections due to CO_2 in the exhausted gases are normally included. This technique has gained considerable support and there are now more than 30 laboratories working with large-scale oxygen consumption calorimeters [5].

In tunnel fires similar principles may be utilised by measuring the flow and oxygen profiles over a cross-section at both sides of the fire. Air is drawn to the fire in the lower part of the tunnel whereas hot fire products flow from the fire in the upper part. By integrating mass flow rates and oxygen consumption, the heat release rates can be determined. The greatest advantage with this technique is its ability to measure very large heat release rates (> 10 MW) with an reasonable accuracy. A large number of measuring probes are, however, required.

3 Experimental Set-up

The tunnel used for the experiments was a 2.3 km long abandoned copper-mine. In Figure 1 the main layout of the tunnel is shown.

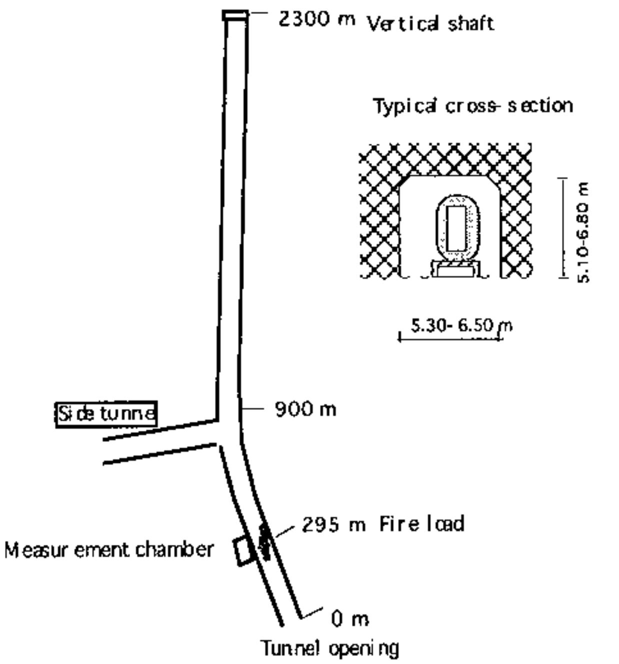

Figure 1 The tunnel used in the test series was an old copper-mine in North-Norway. The tunnel is 2.3 km long and the burning vehicles were located 295 m from the tunnel opening. The figure shows a layout and a typical cross-section of the tunnel.

The surface of the tunnel was very rough but for approximately 70 m of each side of the fire a 0.1 m thick concrete was sprayed over the walls to prevent rocks from falling and to make the tunnel surface smoother. The burning vehicles were located 295 m from the opening of the tunnel .

The instrument stations for the mass flow rate measurements were located +34 m and -27 m, respectively, from the centre of the fire (see Figure 2). Three insulated steel piles were mounted at each instrument station. The insulation was made of

Kaowool to protect the plastic pipes and thermocouples connected to the measuring probes. In Figure 2 the locations of the instrument stations are shown. At the centre line piles a dense net of bi-directional probes and thermocouples were mounted.

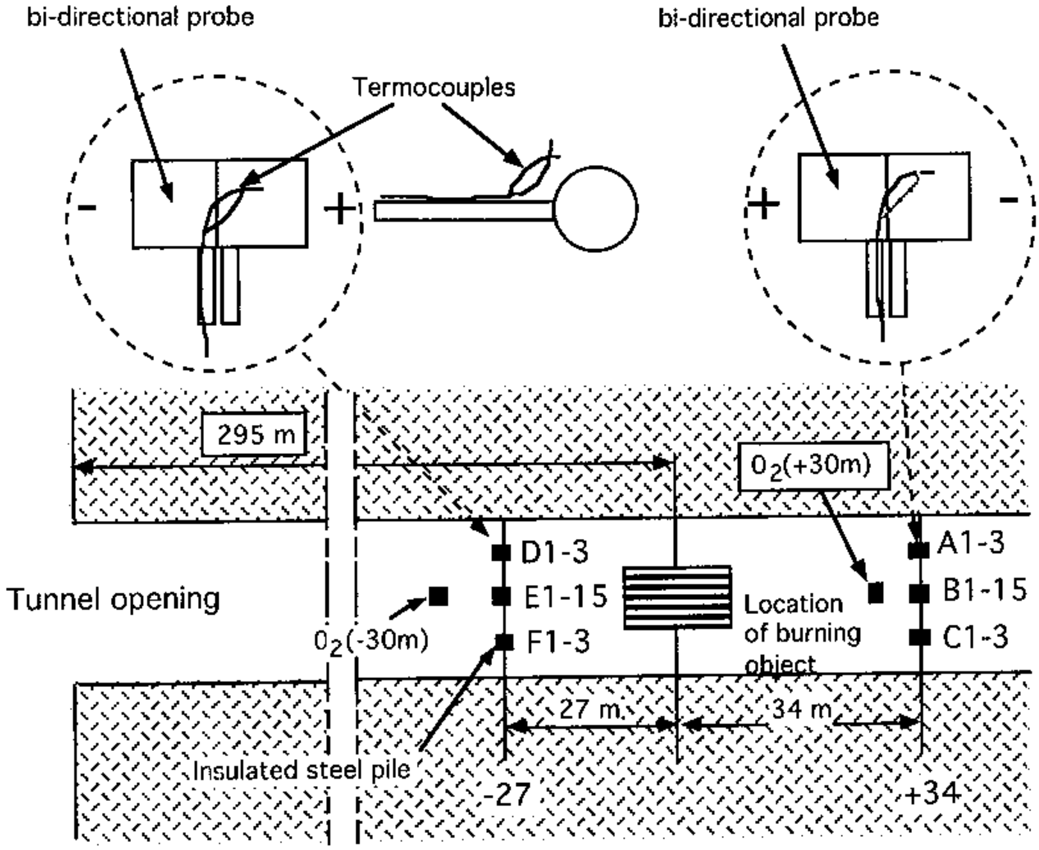

Figure 2 The figure shows the location of the instrument stations in relation to the fire load. Each instrument station consisted of 3 insulated steel piles on each side of the fire. At instrument station -27 m and +34 m, respectively, both bi-directional probes and thermocouples were used to determine the mass flow rate over the cross-section. Three oxygen probes were mounted at +/- 30 m from the fire.

To each bi-directional probe, a type K thermocouple with a wire diameter of 0.25 mm, was attached. The diameter D of the bi-directional probe was 16 mm and the length L was 32 mm. The data were collected in a data acquisition system. The temperature was recorded every 10 second by a 3530 ORION Data Logging System and stored on a Macintosh Power Book portable computer. The pressure difference for the velocity measurements was recorded using two pressure scanners and the data was stored on PC's. The pressure scanners had quite different scanning times. For the faster scanner it took 23 seconds to scan 21 probes and 61 seconds for the slower one. The faster scanner was used to scan probes number

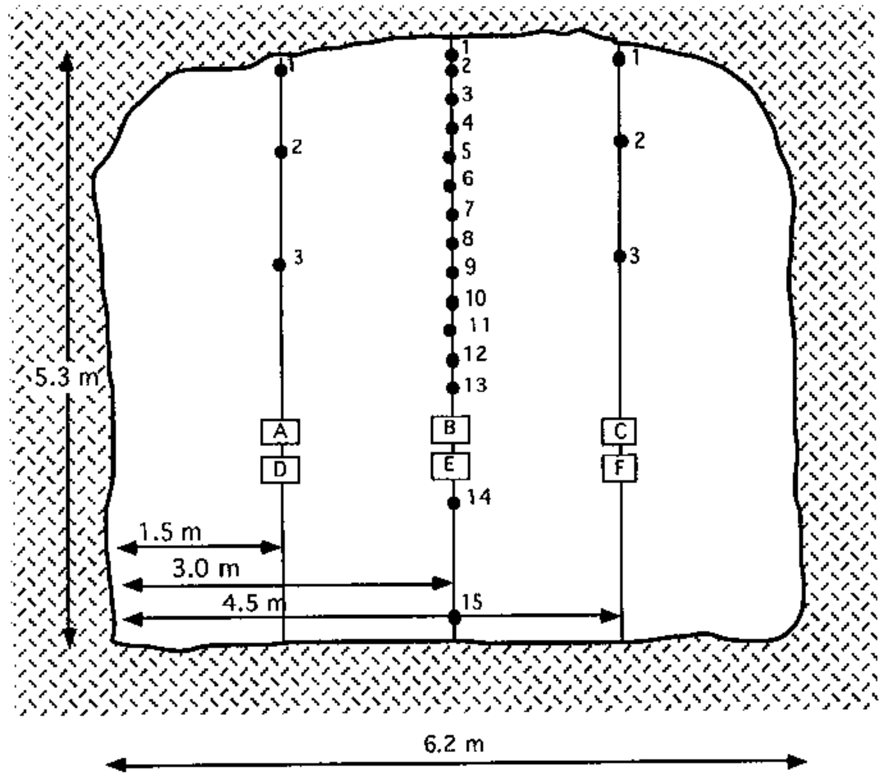

Figure 3 The figure shows a cross-section at instrument station +34 m. On three insulated steel piles bi-directional probes and thermocouples were mounted. Piles A,B and C were at station +34 m and piles D,E and F were at station -27 m. In table 1 the height of each probe from floor level is given for each pile. The ceiling heights used in the calculations were 5.3 m (at +34m) and 5.65 m (at -27 m) respectively and the tunnel widths 6.2 m.

Table 1 Location of temperature and pressure probes at stations -27 m and +34 m

Station +34 m (ceiling height 5.3 m)		Station -27 m (ceiling height 5.65 m)	
point nr.	m from floor	point nr.	m from floor
A1	4.97	D1	5.04
A2	4.22	D2	4.29
A3	3.22	D3	3.29
B1	5.09	E1	5.45
B2	5.01	E2	5.37
B3	4.76	E3	5.12
B4	4.51	E4	4.87
B5	4.26	E5	4.62
B6	4.01	E6	4.37
B7	3.76	E7	4.12
B8	3.51	E8	3.87
B9	3.26	E9	3.62
B10	3.01	E10	3.37
B11	2.76	E11	3.12
B12	2.51	E12	2.87
B13	2.26	E13	2.62
B14	1.26	E14	1.62
B15	0.26	E15	0.62
C1	5.05	F1	5.30
C2	4.30	F2	4.55
C3	3.30	F3	3.55

2-12 (see Figure 3) at the centre line pile on each side. The slower one was used to scan over the three lowest probes (number 13-15) at the centreline pile and the probes on the sides. All the measured data was interpolated with an 10-second interval in order to link temperature, velocity and oxygen files to one common data file.

The oxygen measurements were carried out by using two oxygen analysers of type PMA 10 from M & C Instruments. Three measuring probes, which consisted of open copper tubes (Ø 6 mm) were located at different heights in the cross section at instrument stations +/- 30 m. This location was chosen since the CO_2 data, measured by the Institut für Baustoffe, Massivbau and Brandschutz (IBMB), Germany, was used in the heat release rate calculations presented in chapter 4.2. IBMB measured the CO_2 concentration 0.7 m below the ceiling and 2 m above floor level. A special switch box controlling a system of valves, was designed to read one probe at a time. Each probe was open in 30 seconds and a registration of the oxygen concentration was carried out by the ORION Logger every 10th second. The total scanning time was 1.5 minutes for three probes.

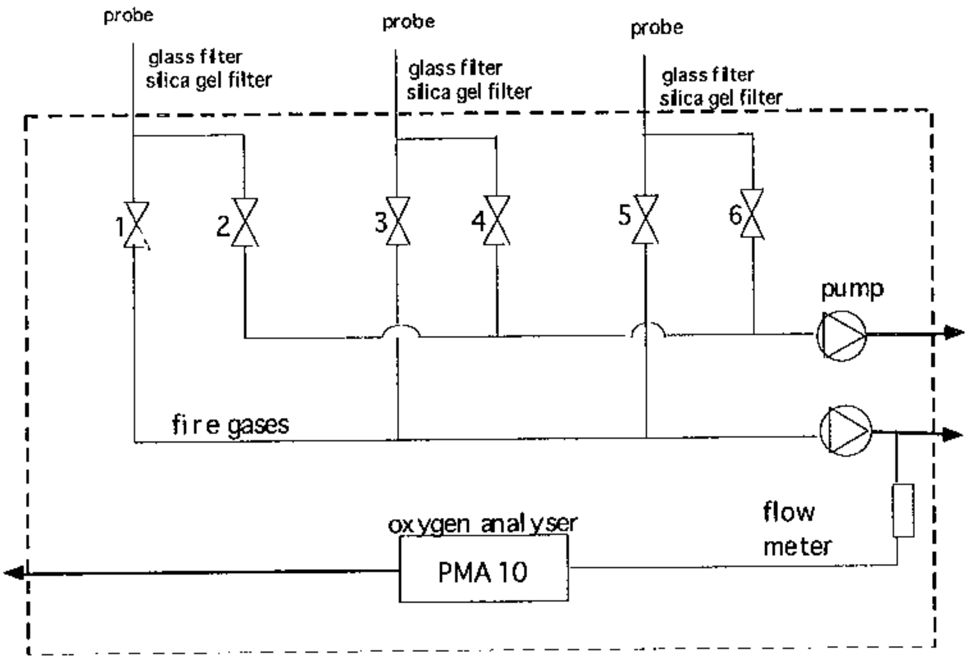

Figure 4 Schematic figure of the oxygen measuring system at one instrument station. Each oxygen analyser was connected to measuring probes at three different levels below the ceiling at the centre of the tunnel cross section, i.e. 0.7 m, 1.4 m and 2.3 m, respectively.

In Figure 4 a schematic figure of the oxygen measuring system, at one measuring station, is shown. Each oxygen analyser was connected to three measuring probes, located 0.7 m, 1.4 m and 2.3 m, respectively, below the ceiling. For example when measuring at the highest located probe, valves number 1, 4 and 6 were open while valves number 2, 3 and 5 were closed during a period of 30 seconds. After 30 seconds valves number 3, 2 and 6 were opened and valve number 1, 4 and 5 were closed etc. The ceiling heights used in the calculations of the heat release rates were 5.3 m at instrument station +34 m and 5.65 m at instrument station -27 m and the width of the tunnel used at both instrument stations was 6.2 m. Corresponding ceiling heights were assumed at instrument stations +/- 30 m. The geometrical measures at the instrument stations were somewhat uncertain since the form of the cross section is rather complex.

4 Calculation of heat release rate (HRR)

In a fire laboratory test the hot gas from the fire is collected by a hood placed above the fire. The hot gas is sucked into a duct system where it is mixed before it is analysed. In the case of a tunnel fire the tunnel in itself is formed as a duct. Thus, the mass flow rate and oxygen concentration profiles can be measured by using a dense net of measuring probes. In a forced duct flow in a laboratory the exhaust gases are well mixed so that a single-point measurement is usually sufficient. In a tunnel, however, the exhaust gases are not well mixed (see Figure 5 to 7), which requires multi-point measurements. Furthermore the exhaust gases are normally severely diluted with cold air above the fire plume whereas in tunnels the dilution is probably small.

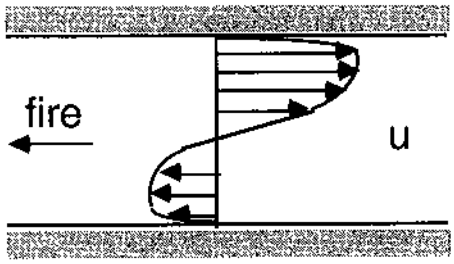

Figure 5 *Typical velocity profiles in tunnel fires without forced ventilation. A stratified counter flow situation usually exist close to the fire source.*

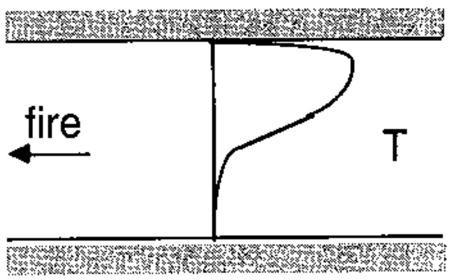

Figure 6 *Typical temperature profiles in tunnel fires without forced ventilation.*

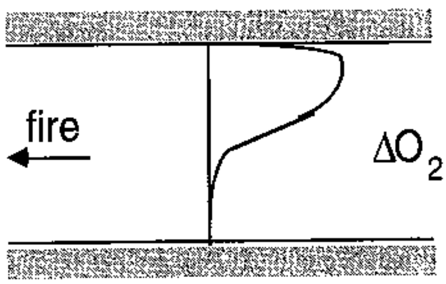

Figure 7 *Typical oxygen deficit profiles in tunnel fires without forced ventilation*

The oxygen concentrations and the mass flow rates have been measured and determined in the exhausted gases. The location was chosen so the flow field would be relatively well established.

4.1 Determination of the mass flow rate

The mass flow rate was determined with aid of a dense net of thermocouples and bi-directional probes covering the cross section at both sides of the fire. In Figure 8 it is shown how the cross-section at instrument station + 34 m was divided into a number of segments, where every segment was related to a measuring point (filled circles). Corresponding division was made at instrument station -27 m. The velocity probes were mounted denser in the upper part of the cross-section as the flow variation was expected to be greater there.

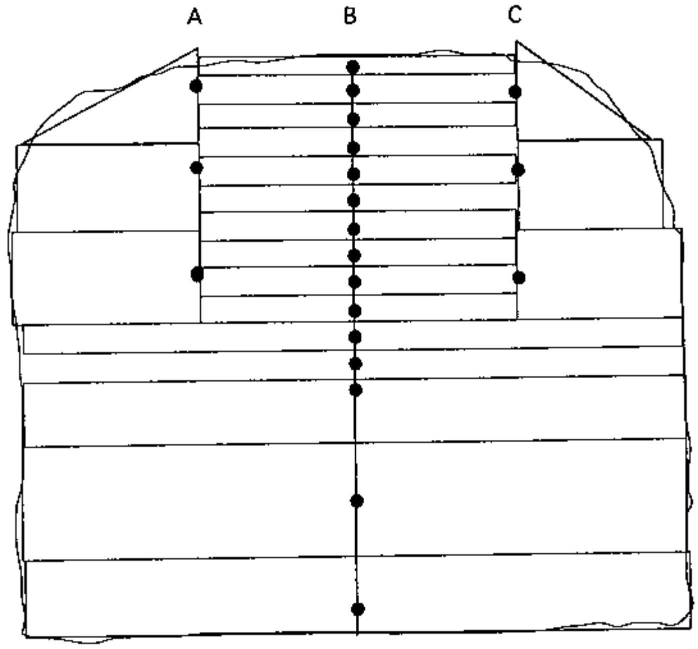

Figure 8 The figure shows the division of the tunnel cross-section at instrument station +34 m into different area segments. The mass flow rate was calculated for each segment and the total mass flow rate was determined by summing up them.

The mass flow rate per unit area was determined according to the following equation:

$$\dot{m}''_k = \rho_k u_k = \frac{T_0 \rho_0}{T_k} u_k \qquad (1)$$

where

$\dot{m}''_k$ = mass flow per unit area in measurement point k (kg/s m^2)
u_k = velocity in measurement point k (m/s)
T_k = gas temperature in measurement point k (K)
T_0 = ambient temperature (K)
ρ_0 = density at ambient temperature (K)

The mass flow rate for each segment was determined by multiplying the area with the values obtained from equation (1) and a theoretically determined mass flow correction factor, ζ_k, a factor accounting for the variation of temerature and velocity over the segment. The correction factor is depending on location and gas temperature. Velocity and gas temperature difference profiles (ΔT) were assumed to follow a one-seventh-power relation for turbulent boundary layer flow (the Prandtl number is assumed to be one here). An average factor of 0,97 (for gas temperatures in the range 0 to 300 °C) was obtained for the "short" centreline segments and a coefficient of 0,91 for others. Thus, if the tunnel cross-sectional area is divided into n segments ΔA_k, the total mass flow rate was obtained with aid of the following equation:

$$\dot{m}_e = \sum_n \zeta_k \Delta A_k \dot{m}_k'' \qquad (2)$$

A distinction was made between outflowing (exhausted) and inflowing gases by examining the signs of the measured velocity. Only positive signs of the velocity, i.e. exhaust gases in the cross-section, were used to calculate the total mass flow rate, $\dot{m}_e$, in equation (2).

The velocity u was determined with aid of the measured dynamic pressure difference Δp at each probe and the corresponding temperature. The velocity was obtained from equation (3):

$$u = \frac{1}{k(\mathrm{Re})}\sqrt{\frac{2\Delta p T}{\rho_0 T_0}} \qquad (3)$$

where k (Re) is a correction coefficient given by McCaffrey and Heskestad [9] which depends on the Reynolds number (Re). This coefficient is nearly constant for Re>3800 or k (Re) ≈ 1.08. This value was used in the calculation of the velocity. For Reynolds numbers 40 < Re < 3800, k (Re) can increase from 1.08 to about 1.3. This has not been taken into account which leads to overestimated results as k (Re) appears in the denominator of equation (3). The ambient values used in equation (3) were T_0 = 276 K (3 °C) and ρ_0=1.27 kg/m^3.

In Figure 9 to 12 the temperature and velocity profiles are shown at both instrument stations (-27 m and +34 m) from a test with a passenger train. These are the maximum values from the fire test with the passenger train. The calculated heat release rate is 12 MW and the time from ignition is 104 minutes.

Figures 9 to 12 can be used to calculate the mass balance. A rough calculation demonstrates the mass balance, i.e. the hot gases flowing out are approximately the same as the gases flowing in, or nearly 25 kg/s.

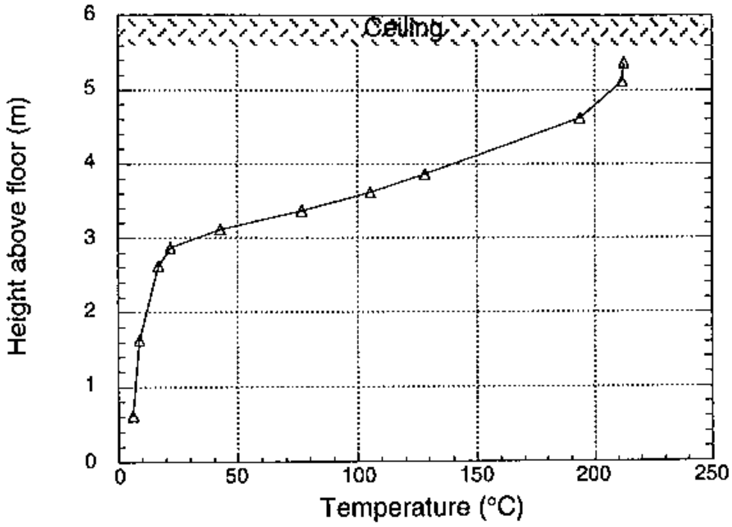

Figure 9 Measured temperature profile at measuring station -27 m after 104 minutes from ignition. The fire load is a train and the calculated heat release rate is 12 MW.

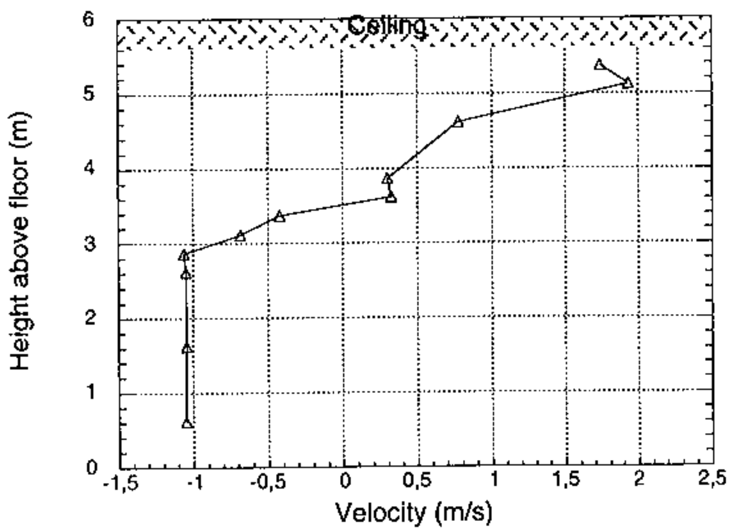

Figure 10 Measured velocity profile at measuring station -27 m after 104 minutes from ignition. Negative velocity corresponds to an inflow of gas.

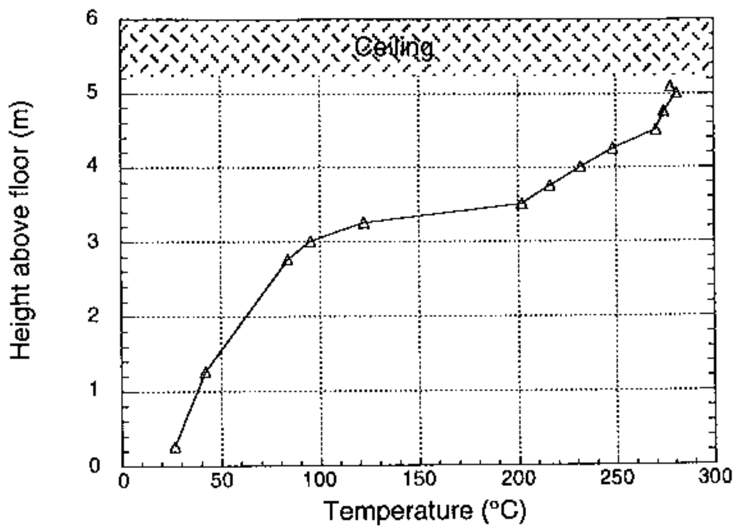

Figure 11 Measured temperature profile at measuring station +34 m after 104 minutes from ignition.

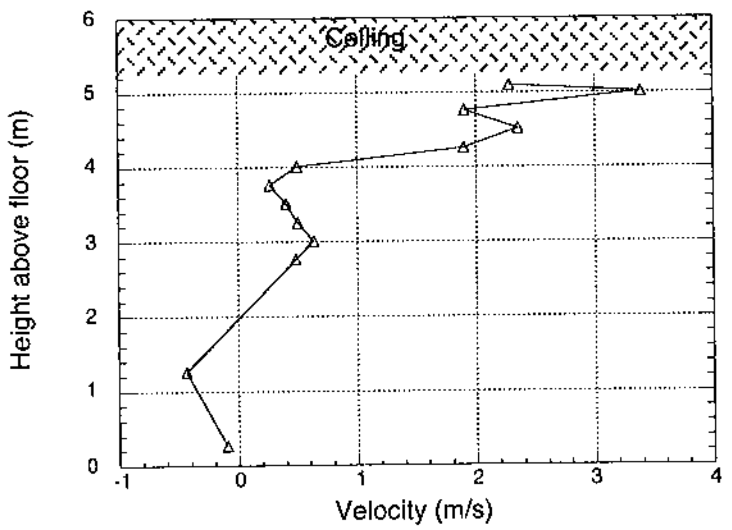

Figure 12 Measured velocity profile at measuring station +34 m after 104 minutes from ignition. Negative velocity corresponds to an inflow of gas.

4.2 Determination of heat release rate

Equation (4) was used for calculation of the total heat release rate (HRR). The equation includes corrections for CO_2 and H_2O [10]:

$$HRR = E\frac{\phi}{1+\phi(\alpha-1)}\dot{m}_e\frac{M_{O2}}{M_a}\left(1-X^0_{H2O}-X^0_{CO_2}\right)X^0_{O2} \tag{4}$$

where

$$\phi = \frac{X^0_{O2}\left(1-X_{CO2}\right)-X_{O2}\left(1-X^0_{CO2}\right)}{X^0_{O2}\left(1-X_{O2}-X_{CO2}\right)}$$

and

E	= heat released per unit mass of O_2 consumed, 13.1 MJ/kg of O_2
$X^0_{O_2}$	= measured mole fraction of O_2 in the inflowing gases
X_{O_2}	= measured mole fraction of O_2 in the exhausted gases
$\dot{m}_e$	= mass flow rate of the exhausted gases (kg/s)
M_{O2}	= molecular weight of O_2, (32 kg/kmol)
M_a	= molecular weight of the inflowing gases, (29 kg/kmol)
$X^0_{H_2O}$	= mole fraction of H_2O in the inflowing gases
X_{CO_2}	= measured mole fraction of CO_2 in the exhausted gases
$X^0_{CO_2}$	= measured mole fraction of CO_2 in the inflowing gases
$\alpha \approx 1.1$	

This equation is usually used for calculation of heat release rates in laboratory calorimeters. The inflowing air is normally at ambient conditions ($X^0_{O_2}$ =0.2095, $X^0_{CO_2}$ <0.00033, $X^0_{H_2O}$< 0.005) but in most of the tests the incoming air in the lower part of the cross section was found after a while (<10 min) to contain higher concentration of CO_2 (in the order of 0.5-1 %) than in normal air and thus lower concentration of O_2. This problem was considered here by using the measured $X^0_{CO_2}$ value 2 m above floor level (only used when the velocity probes at 2 m indicated inflow of gases) in equation (4) and theoretically calculated mole fraction $X^0_{O_2}$ since the O_2 concentration was not measured 2 m above floor level. The theoretically calculated mole fraction of the inflowing gases was obtained by the following equation:

$$X^0_{O2} = \left(\frac{X_{CO_2}-X^0_{CO_2}}{X_{CO_2}}\right)0{,}2095+\left(\frac{X^0_{CO_2}}{X_{CO_2}}\right)X_{O2} \tag{5}$$

where $X^0_{CO_2}$ here is the measured mole fraction of CO_2 in the inflowing gases.

Equation (6) can be used to demonstrate the effects of different corrections on the HRR. We first neglect the effect of $X^0_{H_2O}$ and $X^0_{CO_2}$ as we assume the inflowing gases to be at ambient and then we neglect the corrections due to CO_2 production in the fire. Thus , equation (4) can be simplified to:

$$HRR = E\frac{\phi}{1+\phi(\alpha-1)}\dot{m}_e\frac{M_{O2}}{M_a}X^0_{O2} \tag{6}$$

where

$$\phi = \frac{X_{O2}^{0} - X_{O2}}{\left(1 - X_{O2}\right)X_{O2}^{0}}$$

The HRR was calculated by summing up the mass flow rates (three different groups), each belonging to a certain oxygen probe, as shown in Figure 13 (filled circle). The mass flow rate groups are indicated by a specific pattern of the segments in Figure 13. Only positive mass flow rates were used in the calculation.

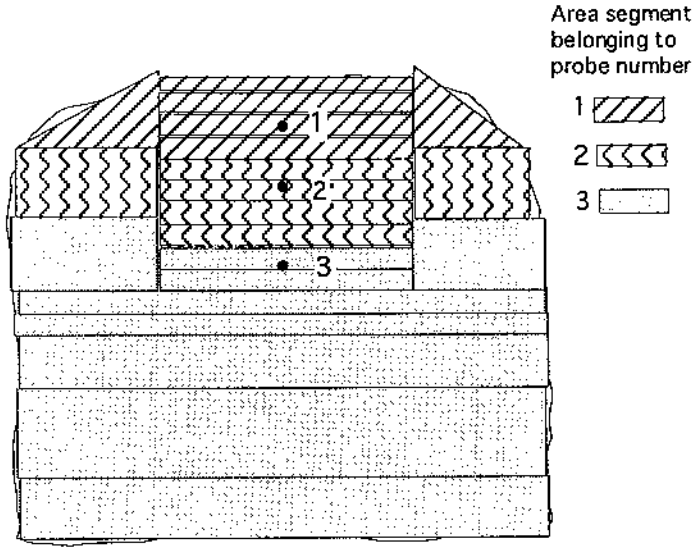

Figure 13 The HRR was calculated by summing up the mass flow rates each belonging to a certain oxygen probe. Only the positive mass flow rates were used.

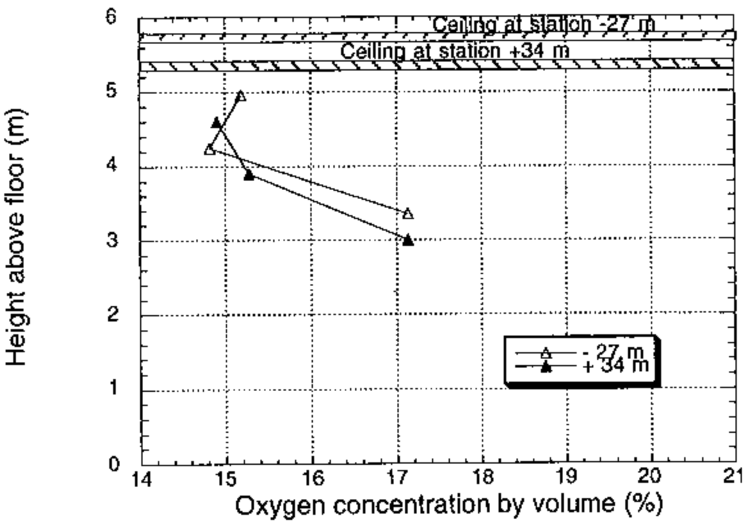

Figure 14 Oxygen concentration at measurement station -27 m and + 34 m, respectively, after 104 minutes from ignition. The fire load is a passenger train.

In Figure 14, the oxygen concentration in the three measuring probes, X_{O2} in equations (4) and (6), are shown at both instrument stations at 104 min. The fire load is a passenger train and the calculated heat release rate, according to equation (4) is 12 MW. The general equation for the convective fraction of the total HRR (HRR_{conv}) is given by equation (7):

$$HRR_{conv} = \dot{m}_e \int_{T_0}^{T} c_p(T)dT - \dot{Q}_{loss} \tag{7}$$

where

c_p = specific heat of the exhaust gases

$\dot{Q}_{loss}$ = heat loss before measurements

$\dot{Q}_{loss}$ consists of convective heat loss to the tunnel walls and radiative heat loss from smoke layer to the tunnel walls. This equation can be simplified if c_p is assumed constant (c_p=1000 J/°C kg) and the heat losses are neglected:

$$HRR_{conv} = \dot{m}_e c_p \Delta T \tag{8}$$

where ΔT is the temperature difference ($T-T_0$). T_0 was assumed to be 3 °C but the experiments show that this temperature, i.e. the temperature of the inflowing gases, varies during the fire. Thus, the results obtained by equation (8) and which are presented in Appendix G, are overestimated values.

5 Test results

5.1 Heat Release Rate results

In the following Figures 15 - 20, calculated heat release rates using equation (4) from six tests are presented. In Appendix A-F measured values of temperatures and dynamic pressures are presented. Detailed information about the tested vehicles can be obtained from the technical report for the EUREKA 499 - project [11].

5.1.1 School bus

In the first test, SP measured the total heat release rate (HRR) from a 25-35 year (guess) old VOLVO-schoolbus with 85 seats. In Figure 15 the calculated HRR is shown.

The following measuring points (vel,temp) were missing: A1-3,B13-15,C1-3, D1-3,E13-15 and F1-3 (see Figure 3). In the calculation of HRR the division of the area segments shown in Figure 8 was therefore changed to compensate for the missing points. The test was carried out without any forced ventilation.

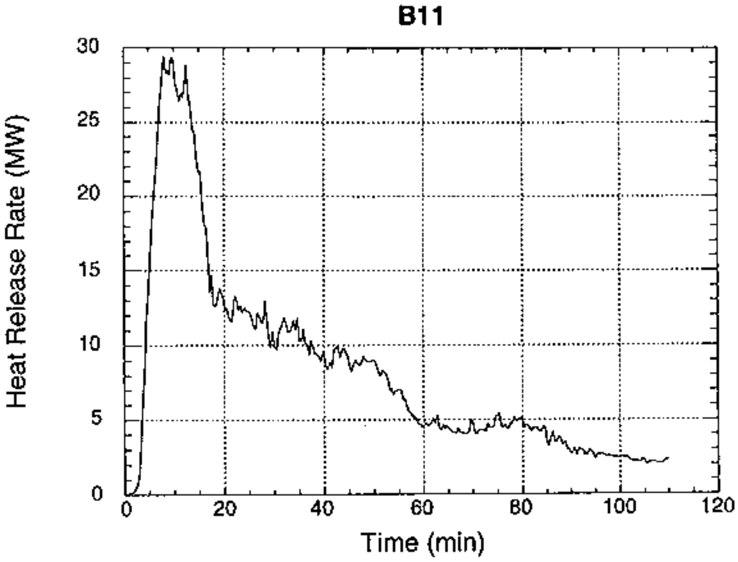

Figure 15 Total heat release rate (HRR) from a test with a schoolbus.

5.1.2 Wood Crib test without forced ventilation

In Figure 16 the HRR is shown for a test with a 950 kg wood crib stack measuring 3.2 m long, 0.8 m wide and 2.4 m high. The density of the wood crib piles was 500 kg/m^3 and they measured 0.04 m wide, 0.04 m thick and 0.8 m long. Thus, the wood crib stack consisted of, by volume, 30% of wood and 70% of air. The test was carried out without any forced ventilation.

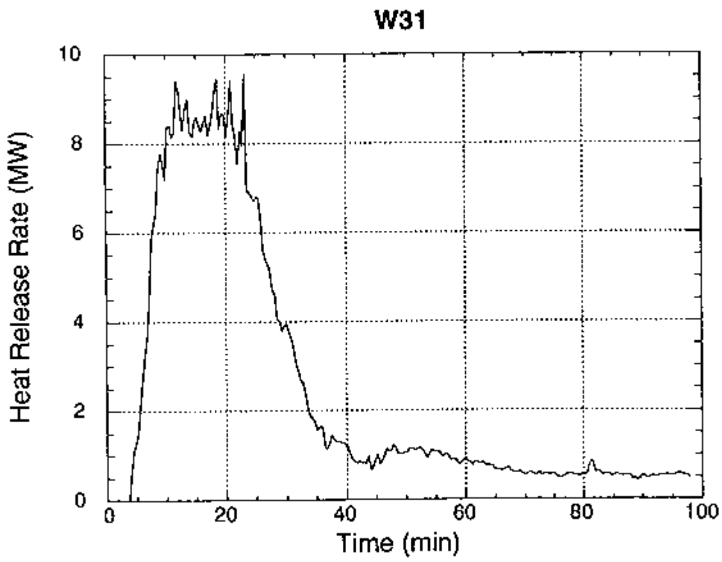

Figure 16 Total heat release rate (HRR) from a test with a wood crib without fans.

5.1.3 Wood Crib test with forced ventilation

In Figure 17 the HRR is shown for a 950 kg wood crib stack with forced ventilation. The wood crib stack collapsed after about 18 minutes.

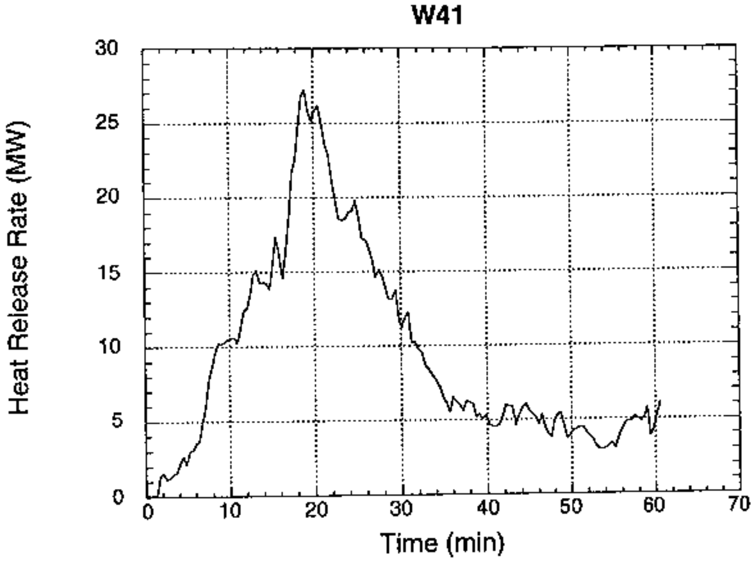

Figure 17 Total heat release rate (HRR) from a test with a wood crib with forced ventilation (average velocity=2.9 m/s).

This test was carried out with longitudinal ventilation where the average velocity over the cross-section was 2.9 m/s. No temperature or velocity changes were registered at the upstream instrument station (-27 m). This means that all the heat and smoke was blown in the direction of the air flow. The fan, which was an axial flow fan of type PSC, 450 kW, was placed in a cabin at the tunnel entrance (-295 m).

5.1.4 Passenger train

In Figure 18 the HRR is shown for a German passenger train (Inter City train). The passenger train was 20.6 m long, 2.7 m wide and 3 m high. The number of seats was 80 and the total heat content of the seats was nearly 9000 MJ. The total heat content for the train was calculated to be 77 000 MJ [11,12]. As one of the pressure scanners stopped after about 110 minutes the rest of the HRR the curve is based on the CO_2 measurements obtained from IBMB in Germany.

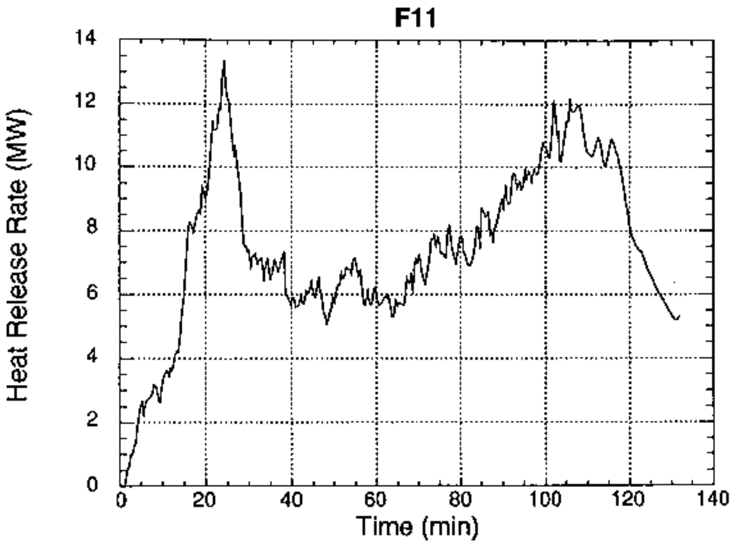

Figure 18 Total heat release rate (HRR) from a test with a passenger train.

5.1.5 Subway Coach

In Figure 19 the HRR is shown for a German subway coach. The subway coach was 18 m long, 2.8 m wide and 3 m high. The number of seats was 40 and they were made of polyurethane foam (totally 210 kg) covered with textiles. The total heat content of the seats was calculated to be 6000 MJ whereas the total heat content of the subway coach was calculated to be 41 300 MJ [11,12].

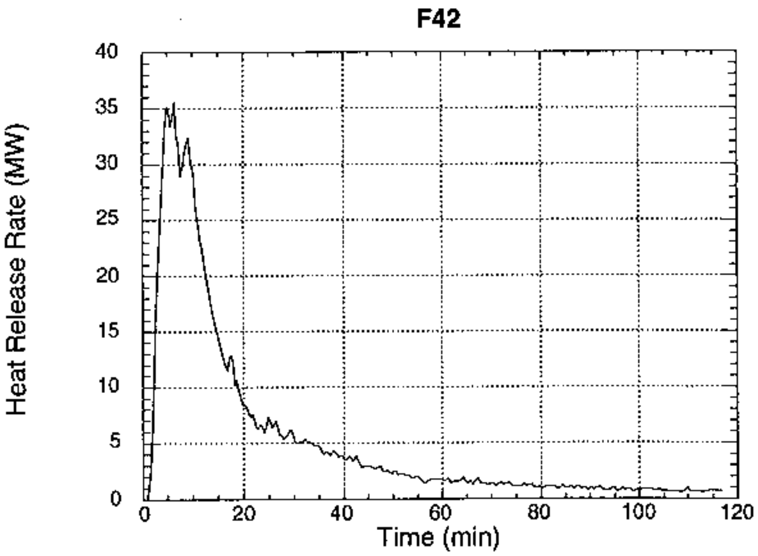

Figure 19 Total heat release rate (HRR) from a test with a subway coach. The pressure tubes and the thermocouple cables for instrument station -27 m were partly damaged. The HRR for - 27 m is reconstructed in accordance to CO_2 measurements.

After about 10 minutes the pressure tubes burned off at instrument station - 27 and after about 25 minutes (see Appendix E) the thermocouple cables for instrument station -27 m were partly damaged because melted aluminium from the subway coach burned through the cable insulation. Therefore we have reconstructed the HRR at - 27 m based on measurements from IBMB.

5.1.6 Simulated truck load

In Figure 20 the HRR is shown for a simulated truck load. The fire load consisted of 2212 kg densely packed wood cribs, 310 kg plastic which was mixed with the wood cribs and 332 kg rubber tiers which were put onto the wood stack. The fire load measured 2.4 m wide, 2.4 m long and about 2.2 m high.

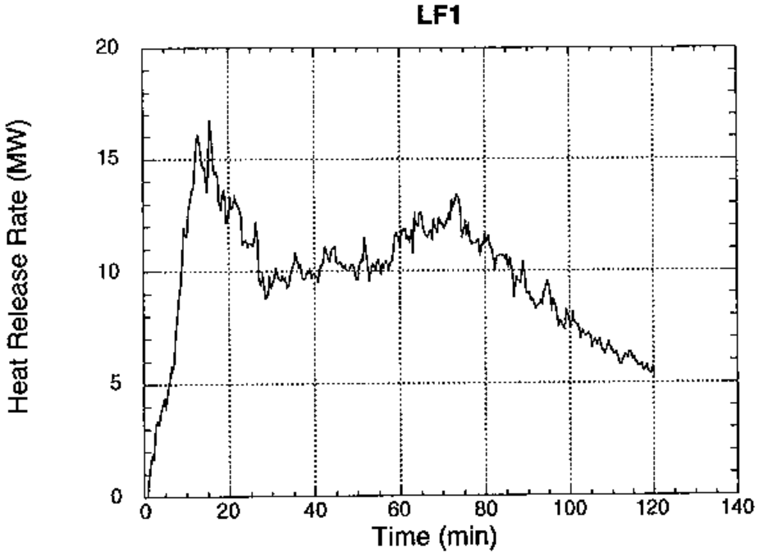

Figure 20 Total heat release rate (HRR) from a test with a simulated truck load.

5.1.7 Integrated heat release rate

The calculated heat release rates curves shown in Figure 15-20 were integrated to make a comparison to the theoretical heat content of each burning object. This comparison can indicate if the order of magnitudes are reasonable. In Table 2, a comparison is made between the integrated HRR and the theoretical heat content. The total heat content for the schoolbus tested is not available but a rough estimation made by the IBMB [12] yield about 48 000 MJ. The information given for the trains was also provided by the IBMB, Germany [11,12].

Table 2 Comparison of theoretical heat content (MJ) and the integrated HRR (MJ) for the measured objects.

Burning object	Time of integration [min]	Maximum HRR value [MW]	Integrated HRR value [MJ]	Theoretical value [MJ]
Schoolbus (B11)	0 - 110	29	29 529	48 000 1)
Wood crib (W31)	0 - 97	9.5	14 354	17 026 2)
Wood crib (W41)	0 - 60	27	33 762	17 026 2)
Passenger train (F11)	0 - 130	13.5	58 490	77 000 3)
Subway coach (F42)	0 - 117	35	36 861	41 300 3)
Truck Load (LF1)	0 - 120	17	69 917	64 495 4)

1) Estimated by IBMB in Germany, [12]
2) 950 kg x 17.922 MJ/kg = 17 026 MJ ; ΔH obtained from Ref. [11].
3) Obtained from IBMB; [11,12]
4) 2212 x 17.922 + 310 x 40 + 332 x 37.505 = 64 495 MJ ; ΔH obtained from Ref. [11] except for the plastics (ΔH assumed 40 MJ/kg).

As can be seen in Table 2 the agreement is reasonably good except for the schoolbus test B11 and the wood crib test W41. The uncertainty of the total integrated heat energy for the schoolbus is much higher than for the other tests. In the case of forced ventilation (W41), where the difference is nearly a factor of two, the most likely explanation is that the HRR is considerably overestimated because the oxygen content is assumed constant below the lowest probe.

Generally, we know that if the vertical oxygen variation is great in the cross section, the accuracy of the calculated HRR is very sensitive to the contribution from each of the oxygen probes. This may influence the accuracy of the method considerably. Also, in the case of natural ventilation the re-entrained gases into the fire plume caused by mixing of gases further upstream, may cause problem with the accuracy of the method. Evenly distributed O_2 and CO_2 probes (and CO if necessary) over the entire cross section are necessary to improve the method. Furthermore, asymmetrically placed probes used to check the horizontal distribution are necessary.

5.2 Corrections for HRR and HRR_{conv} in a tunnel calorimeter

In the following, different corrections in the calculation process are discussed and quantified.

5.2.1 Total heat release rate

We start with an estimation of HRR by using equation (4) for the F11 test (Inter City passenger train) after 104 minutes from ignition. We take into account the high concentration of CO_2 in both the exhausted and the inflowing gases. From figures 9 to 12 we can make a rough calculation of the average mass flow rate $\dot{m}_e \approx 25$ kg/s, and from Figure 14 we can estimate the average oxygen concentration $X_{O_2} \approx 0.16$. From IBMB [11] we obtained measured values of $X_{CO_2} \approx 0.05$ (exhaust gas) and $X^0_{CO_2} \approx 0.008$ (inflowing gas). With aid of equation (5) we get $X^0_{o2} = 0.202$ and by using E=13.1 MJ/kg, $X^0_{o2} = 0.202$, $X_{o2} = 0.16$, $X_{CO2} = 0.05$, $X^0_{CO_2} = 0.008$, $X^0_{H_2O} = 0.005$, $\alpha \approx 1.1$, $\dot{m}_e = 25$ kg/s, $M_{02} = 29$ kg/mol and $M_e = 32$

kg/mol we get HRR = 13.8 MW. This is only 15% higher than the more accurately calculated value 12 MW.

If we only consider the high concentrations of CO_2 in the exhaust gases and neglect the high concentrations in the inflowing gases, we obtain with aid of equation (4) and E=13.1 MJ/kg, X^0_{o2} = 0.2095, X_{o2}=0.16, X_{CO2}=0.05, $X^0_{CO_2}$=0.00033, $X^0_{H_2O}$=0.005, $\alpha \approx 1.1$, $\dot{m}_e$=25 kg/s, M_{O2}=29 kg/mol and M_e=32 kg/mol HRR=17.7 MW. This is about 30% higher than 13.8 MW and thus we get an indication of the effects of an vitiated environment on the heat release rate calculations.

If we neglect the effects of high concentrations of CO_2 in both the exhausted and inflowing gases we obtain with aid of equation (6) HRR=20.7 MW. We used E=13.1 MJ/kg, X^0_{o2} = 0.2095, X_{o2}=0.16, $X^0_{CO_2}$=0.00033, $X^0_{H_2O}$=0.005, $\alpha \approx 1.1$ and $\dot{m}_e$=25 kg/s. This is about 50% higher value than 13.8 MW.

This rough calculation show the importance of using corrections for CO_2 in the calculation of the HRR in both the inflowing and the exhausting gases. Not doing these corrections may lead to an error of about 50 %.

5.2.2 Convective heat release rate

From figure 3 in Appendix G we find the HRR_{conv} to be about 4 MW at 104 minutes for the Inter City passenger train. The corresponding HRR is 12 MW. The ratio HRR_{conv}/HRR is 0.33, where one could expected it to vary between 0.6 and 0.7 [2].

It can be shown by theoretical calculations that the measured convective heat release rate HRR_{conv} at the instrument stations (approximately 30 m from the fire) is about 50 % to 60 % of the HRR_{conv} at the fire. Using a lumped heat transfer coefficient (convective + radiative) of 40 W/°C m^2 as given by Kumar and Cox [19] for gas temperatures higher than 100 °C and using an average gas temperature of 300 °C we can calculate the heat losses to be about 4 MW (2 h C_p B L ΔT = 2x40 x 1000 x 5.5 x 30 x 300). Thus HRR_{conv} at the fire place is 4 + 4 = 8 MW and furthermore HRR_{conv}/HRR=0.67 which is more reasonable than 0.33.

To investigate if HRR_{conv} = 4 MW at the instrument station is a reasonable value we can make a rough estimation using figures 9 to 12. The average mass flow rate is $\dot{m}_e$=25 kg/s, the average gas temperature is about 150 °C and C_p is assumed to be 1 kJ/kg°C. Using equation (8) we obtain HRR_{conv} = 3.7 MW which is 8 % lower than the more accurately calculated value 4 MW. This value is therefore reasonable but correction due to increased temperature of the inflowing gas (see figures 9 and 11, varies between 3 to 65 °C) should also be investigated. This correction is found to be 0.35 MW which is only about 10% of the calculated HRR_{conv} and therefore negligible for this case. However, this may not be the case for other tests as the temperature of the inflowing gases varies between the tests.

6 Conclusions

The heat release rates from burning vehicles and wood cribs were determined with two methods. Firstly, by measuring the temperature, and mass flow rate and thus getting the convective fraction of the heat release rate and secondly, by measuring the oxygen concentration and mass flow rate and thus getting the total heat release rate. The experimental results show that the convective fraction is only 30 to 40 percent of the total heat release rate as compared to an expected value of 60 - 70 percent. This difference is caused by heat losses (convection and radiation) from the hot ceiling jet to the cold walls between the fire source and the measurement stations.

There are number of problems related to the use of the oxygen consumption technique in tunnels which need to be discussed. The vertical variation of temperature, velocity and gas concentration are usually great in stratified counter flow as in tunnels with low degree of ventilation (natural). Thus the method requires many measuring probes to obtain reliable data for the heat release rate calculations. An estimation of the maximum error of the total heat release rate data (see Appendix H) is found to be in the order of ±25 % (relative errors conservatively added) and for comparison, the maximum error of the SP Industry Calorimeter [3], which is used in our fire laboratory to measure up to 10 MW fires, is estimated to be less than ± 16%. To improve the method for tunnel applications a more extensive instrumentation is required, especially the number of gas probes (O_2, CO_2) has to be increased. Only three probes were used in the upper part of the cross section on each side. Based on the experience with this technique the gas probes should also be mounted in the lower part of the cross section as well as eccentric to the centreline.

Another problem with the technique is that the hot fire gases in the upper part will gradually cool and the smoke layer will descend to the floor level further away from the fire and mix with the inflowing air. Thus, there will be a gradual re-entrainment of fire gases and consequently, due to lower oxygen concentrations and higher temperatures than otherwise, the calculated heat release rates will be overestimated if this is not taken into consideration. Thus the O_2 and the CO_2 concentrations must be measured both in the exhausted and the inflowing gases. There is also an uncertainty in the horizontal concentration distribution (assumed constant in the calculations) along with the uncertainty in the position of the oxygen concentration neutral layer. A knowledge about the location of the neutral layer for temperature, velocity and gas concentrations is very important for the method used here.

Comparisons between the total heat energy and the time integrated heat release rate were found to agree reasonably well in most cases. Forced ventilation was found to affect the maximum heat release rate of wood cribs considerably or by a factor of three.

7 Acknowledgement

The project was mainly sponsored by the Swedish Fire Research Board (BRANDFORSK) and partly by the National Rescue Services Board (Räddningsverket) and the Swedish Railway Company (Banverket). They are gratefully acknowledged.

8 References

1. Haack, A., Fire Protection in Traffic Tunnels, Initial Recognitions from Large -Scale Tests, 1st International Conference on Safety in Road and Rail Tunnels, Basel, November 1992.
2. Heskestad, G., Fire Plumes, Fire Protection Engineering, SFPE-handbook, Section 1/Chapter 6.
3. Dahlberg, M., The SP Industry Calorimeter, For rate of heat release measurements up to 10 MW, Swedish National Testing and Research Institute, SP-Report 1992:43.
4. Heskestad, G., A Fire Products Collector for Calorimetry into the MW Range, Factory Mutual Research Corporation, FMRC J.I.0C2E1.RA, June 1981.
5. Babrauskas, V., and Grayson, S.J., Heat Release in Fires, Chapter 1, Elsevier Applied Science, 1992.
6. Thornton, W., The Relation of Oxygen to the Heat of Combustion of Organic Compounds, Philosophical Magazine and Journal of Science, 33, 1917.
7. Hugett, C., Estimation of Rate of Heat Release by Means of Oxygen Consumption Measurements, Fire and Materials, Vol 4, p 61, 1980.
8. Parker, W., Calculations of the Heat Release Rate by Oxygen Consumption for Various Applications, NBSIR 81-2427, National Bureau of Standards, Gaithersburg, MD, 1982.
9. MacCaffrey, B.J. and Heskestad, G., A Robust Bidirectional Low-Velocity Probe for Flame and Fire Application, Combustion and Flame 26, 125-127, 1976.
10. Janssens, M., and Parker, W., Oxygen Consumption Calorimetry, Heat Release in Fires", Elsevier science publishers LTD, 1993.
11. Fire Protection in Traffic Tunnels-Findings from Large-Scale Tests within the EUREKA-Project EU 499 Firetun, Final Technical Report, to be published in early 1995.
12. Privat Communication with Dr. Ing. E. Richter, Institut für Baustoffe, Massivbau und Brandschutz (IBMB).
13. Alpert, R.L., Combust. Science Technology, 11, 197, 1975
14. Wilkinson, D.L., Wood, I.R., J. Fluid Mech., 47, 241, 1971
15. Delichatsios, M.A., Combust. Flame, 43, 1, 1981
16. Delichatsios, M.A., J. Fluid Mech., 93, 241, 1979
17. Drysdale, D.D., Fire Dynamics, J. Wiley and Sons.
18. Holman, J.P., Heat Transfer, McGraw Book Company
19. Kumar, S., and Cox, G., Mathematical Modelling of Fires in Road Tunnels, 5th International Symposium on the Aerodynamics & Ventilation of Vehicle Tunnels, Lille, France:20-22 May, 1985.

Appendix A

Test results: bus test (B11)

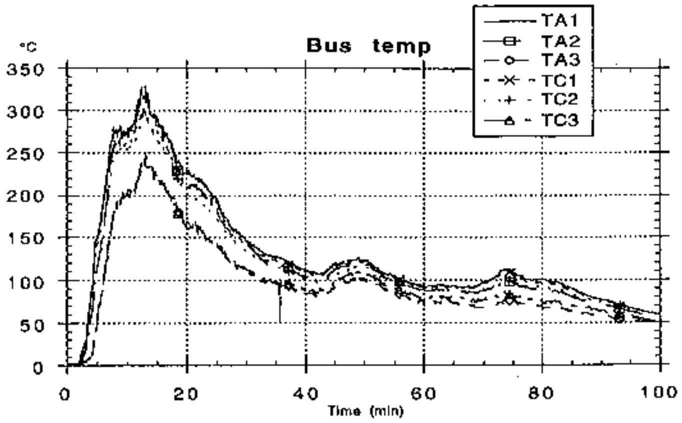

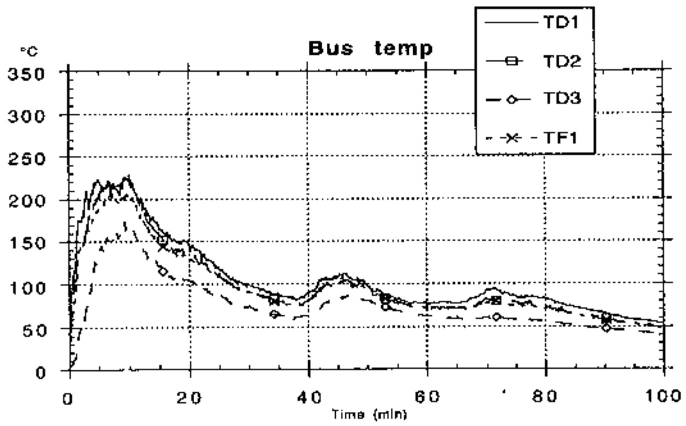

Figure 1. Temperature at instrument-station A, C, D and F.

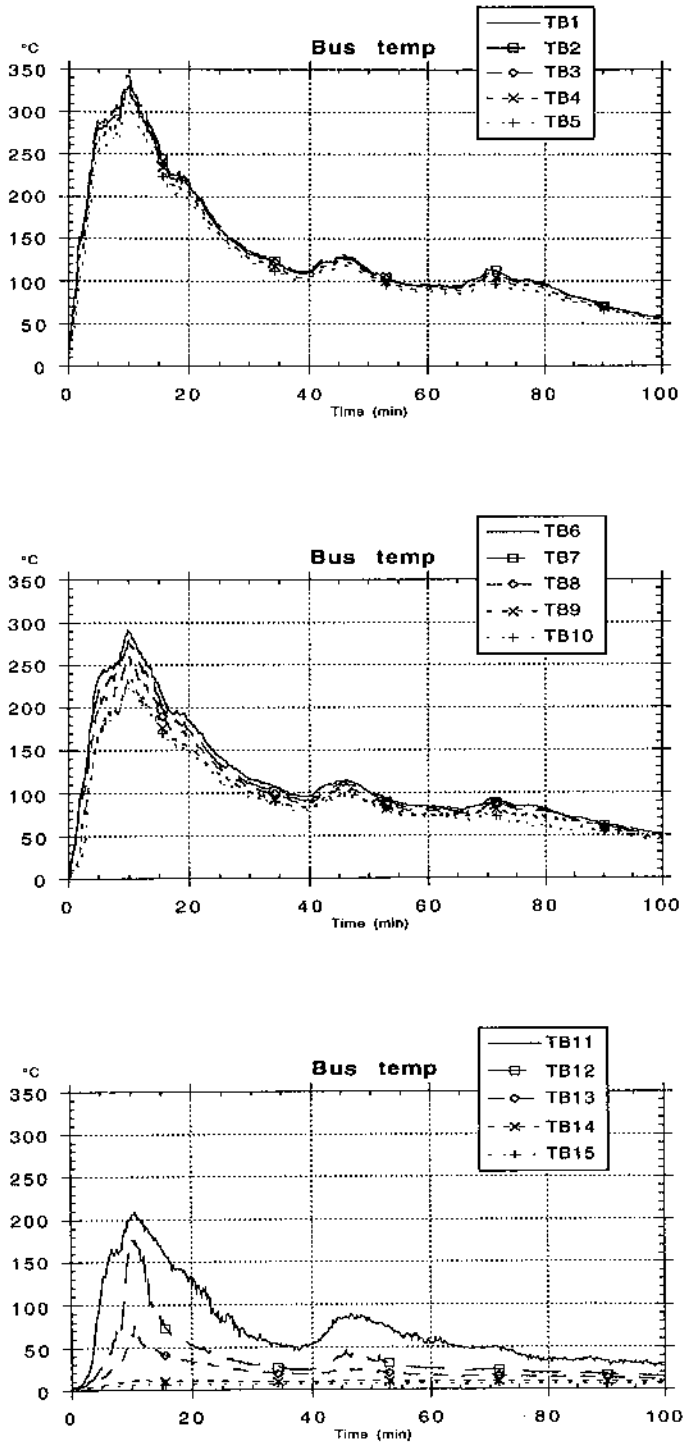

Figure 2. Temperature at instrument-station B.

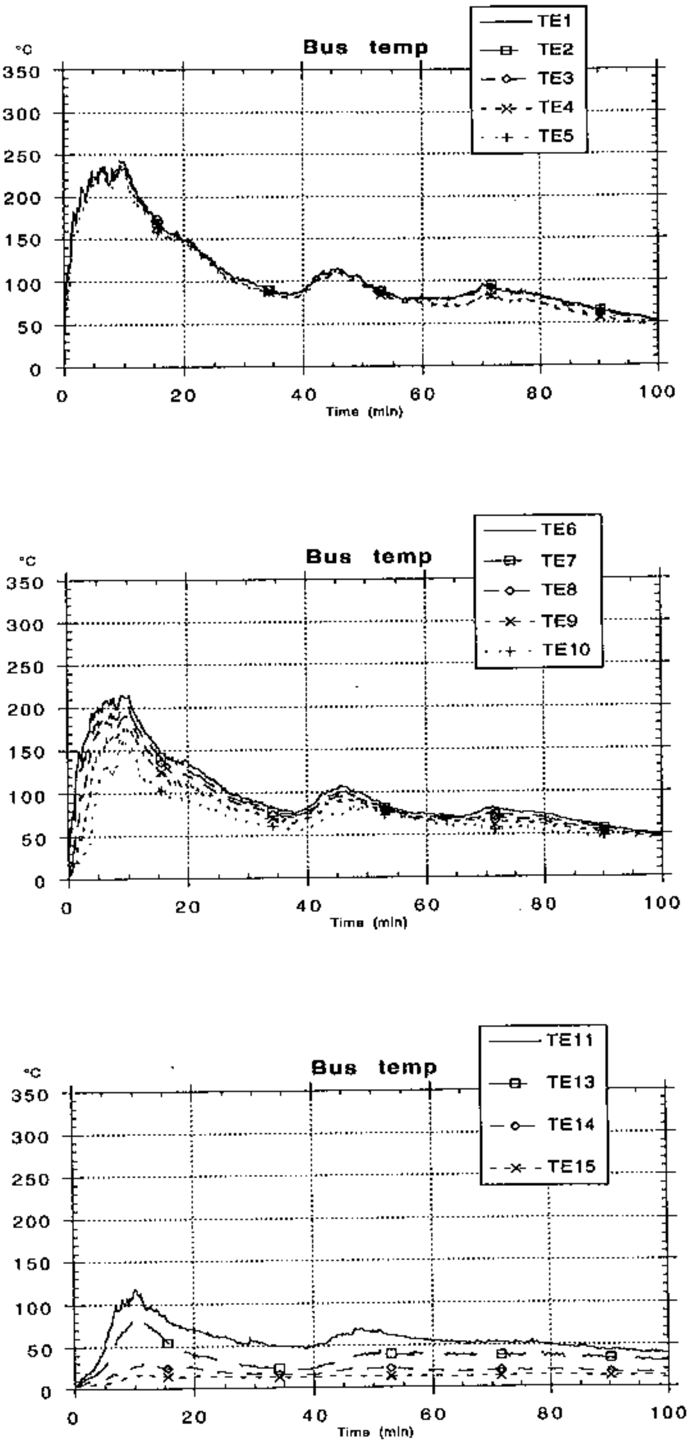

Figure 3. Temperature at instrument-station E.

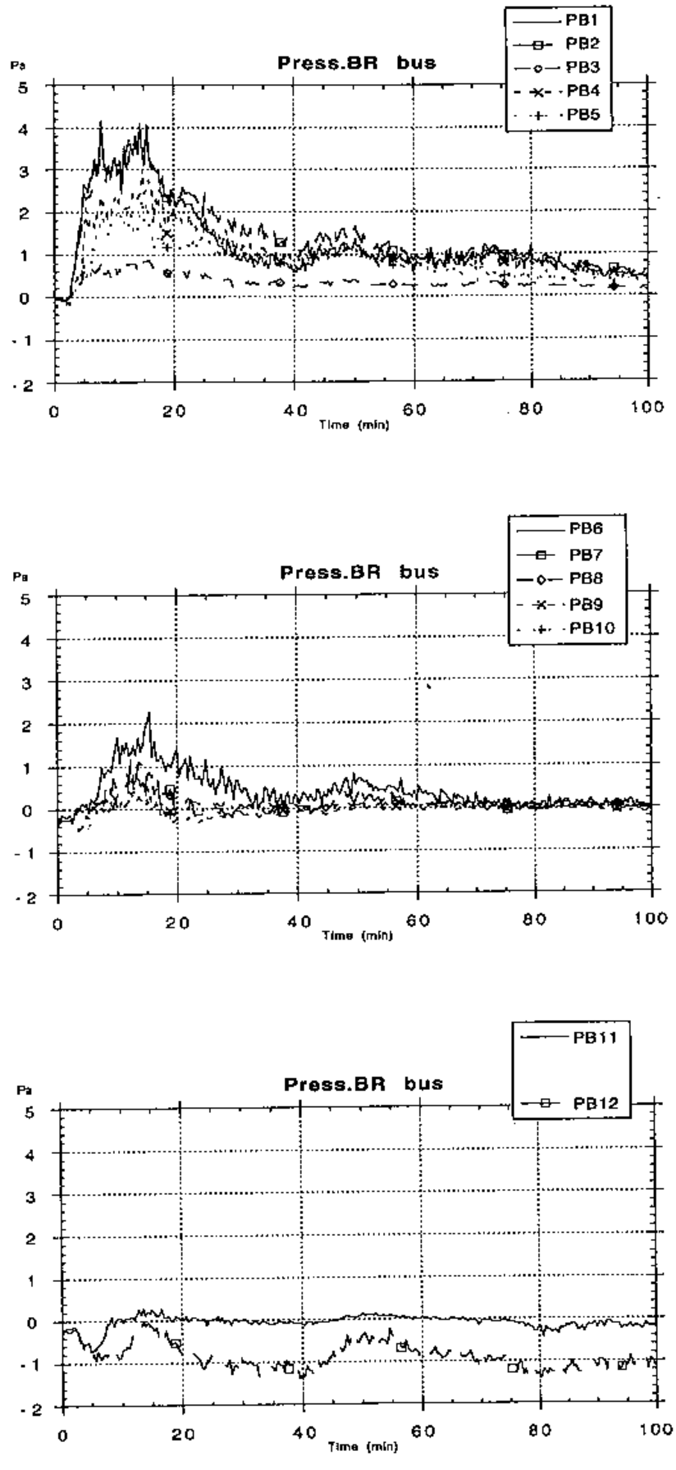

Figure 4. Pressure at instrument-station B.

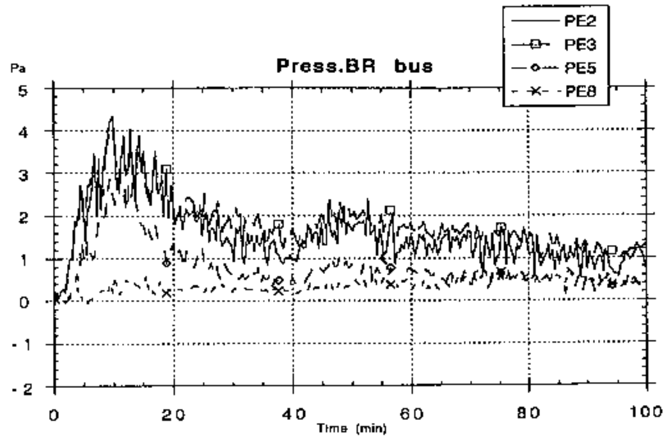

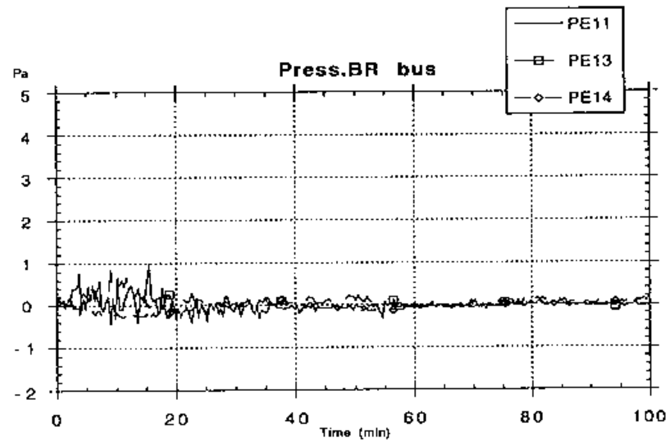

Figure 5. Pressure at instrument-station E.

Appendix B

Test results: wood crib (WC 31)

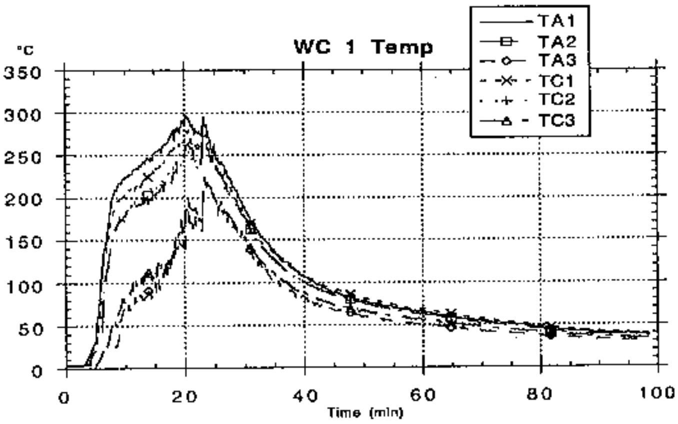

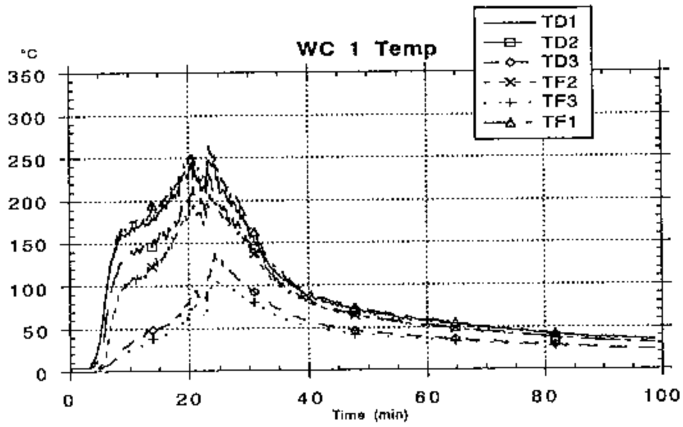

Figure 1. Temperature at instrument-station A, C, D and F.

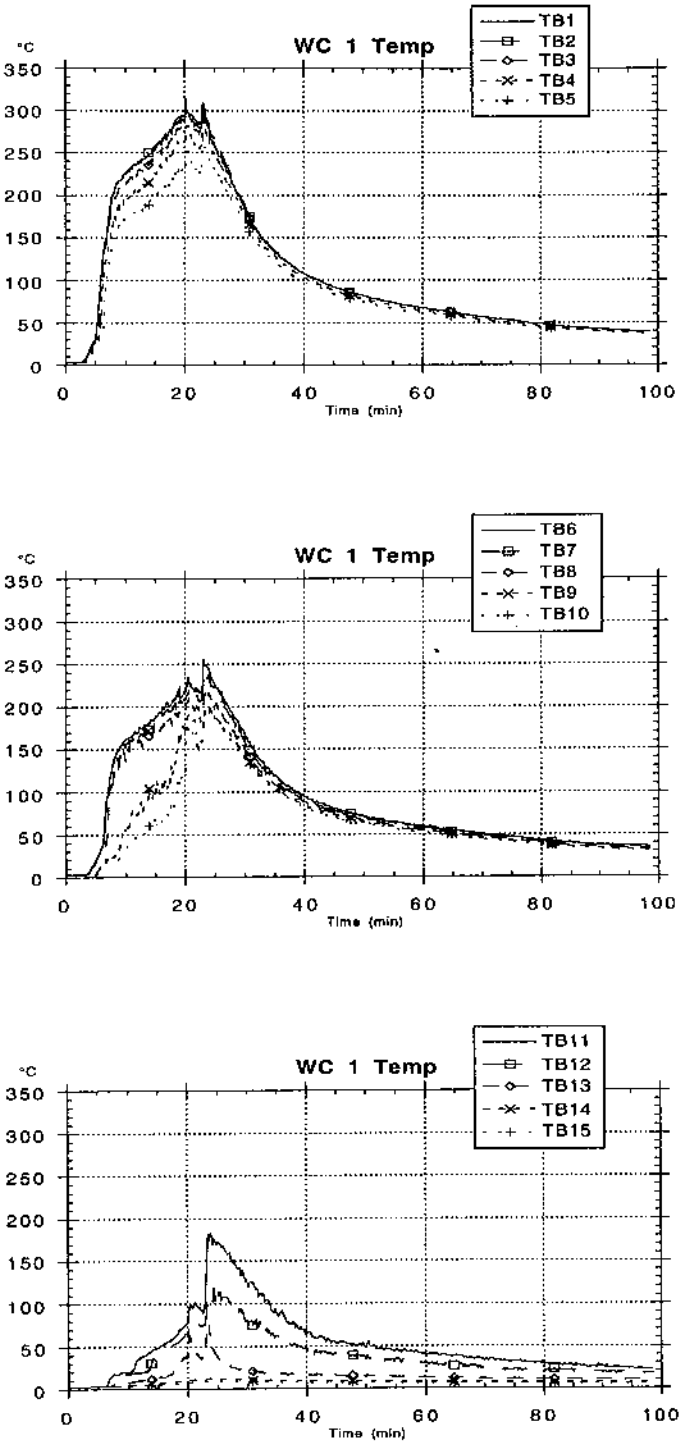

Figure 2. Temperature at instrument-station B.

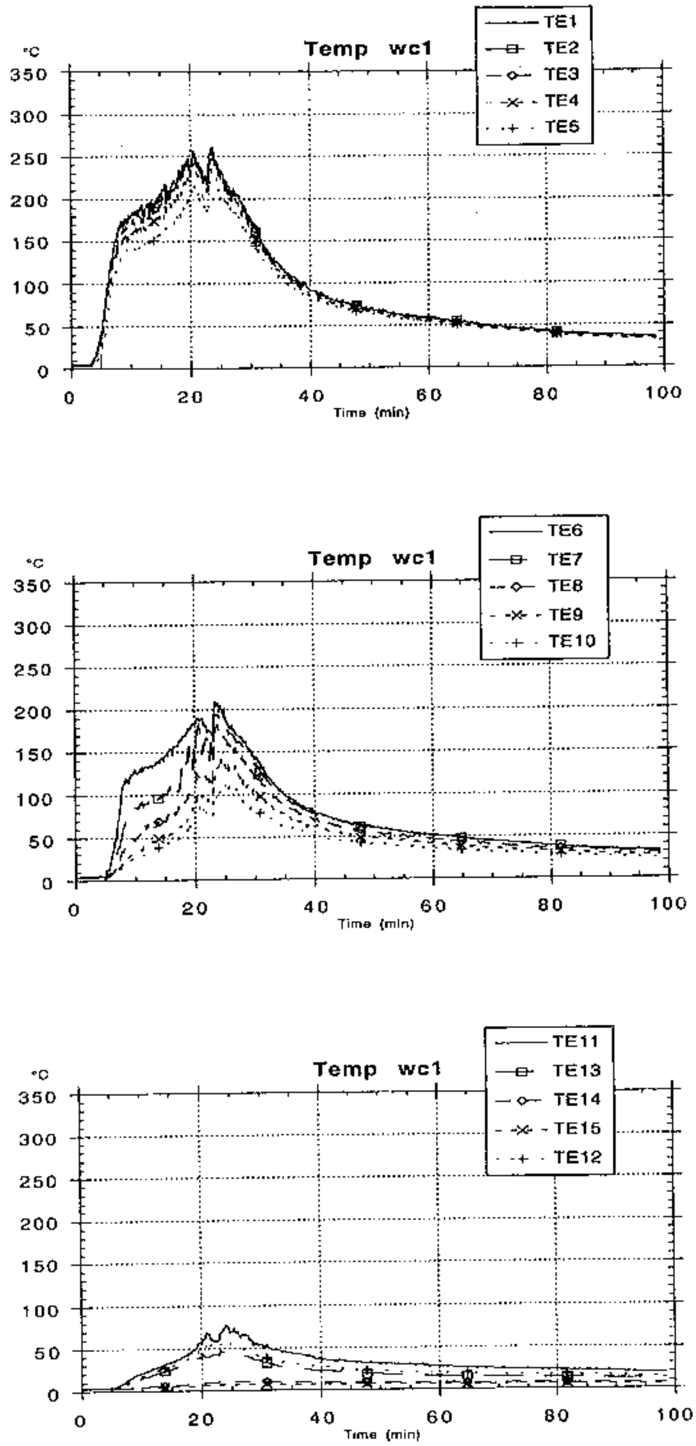

Figure 3. Temperature at instrument-station E.

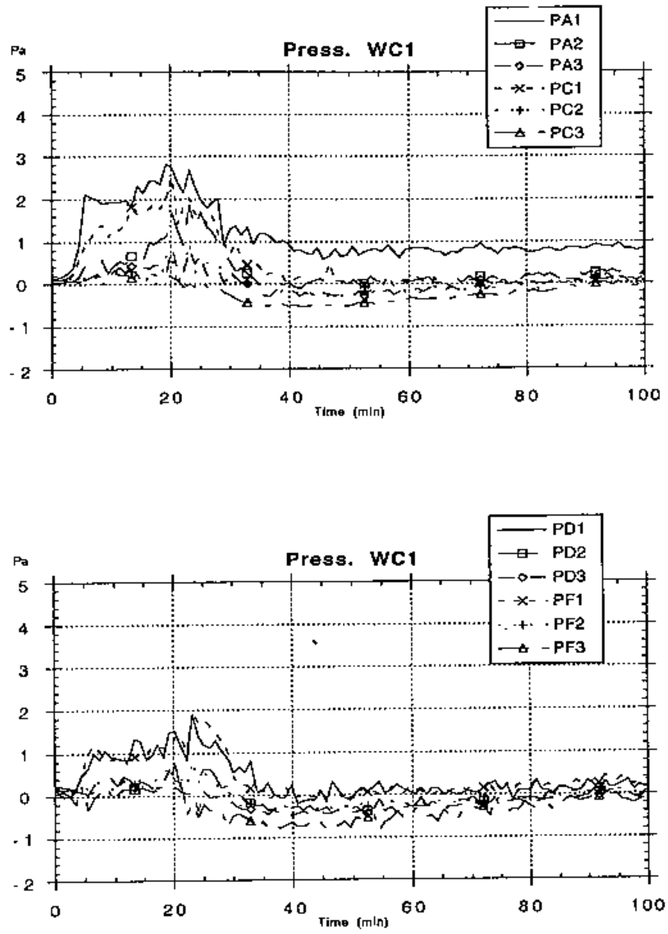

Figure 4. Pressure at instrument-station A, C, D and F.

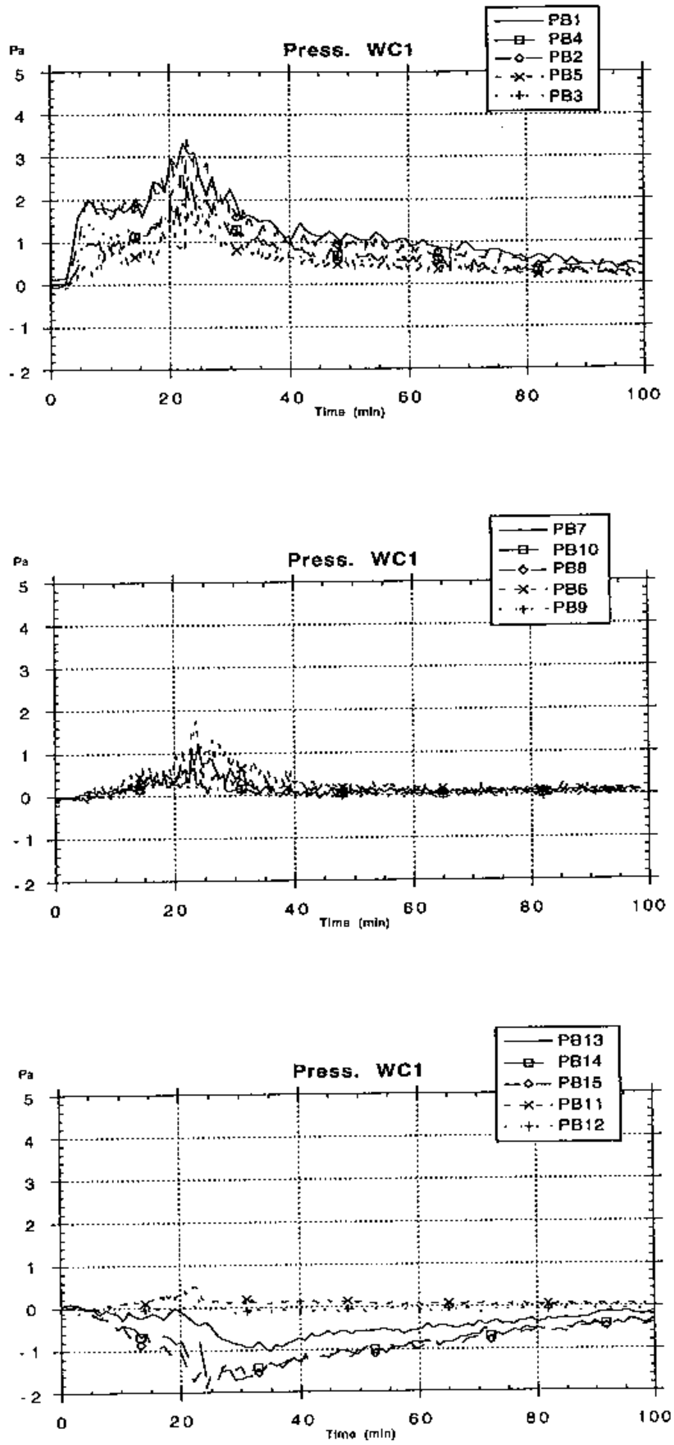

Figure 5. Pressure at instrument-station B.

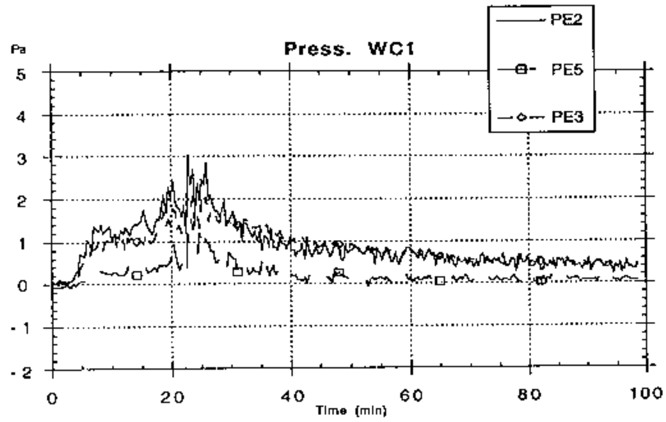

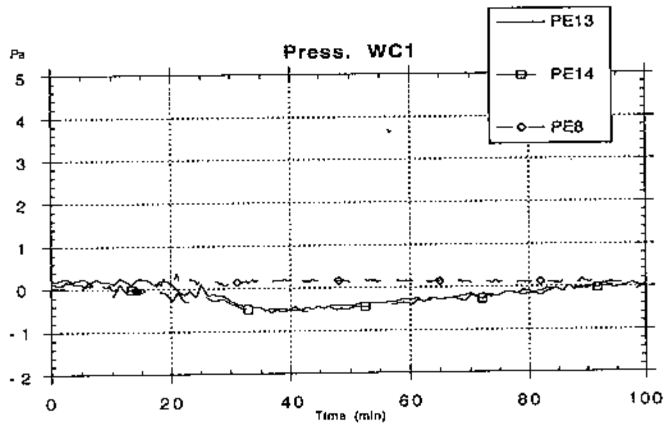

Figure 6. Pressure at instrument-station E.

Appendix C

Test results: wood crib (WC 41)

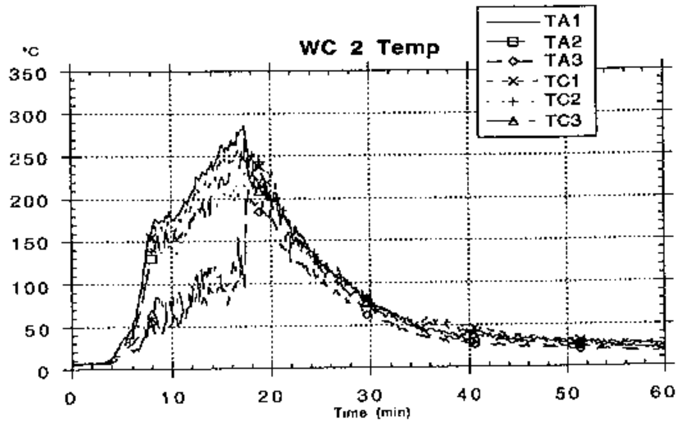

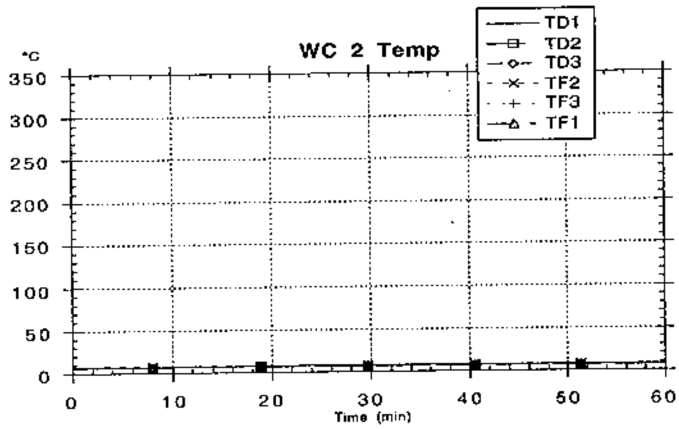

Figure 1. Temperature at instrument-station A, C, D and F.

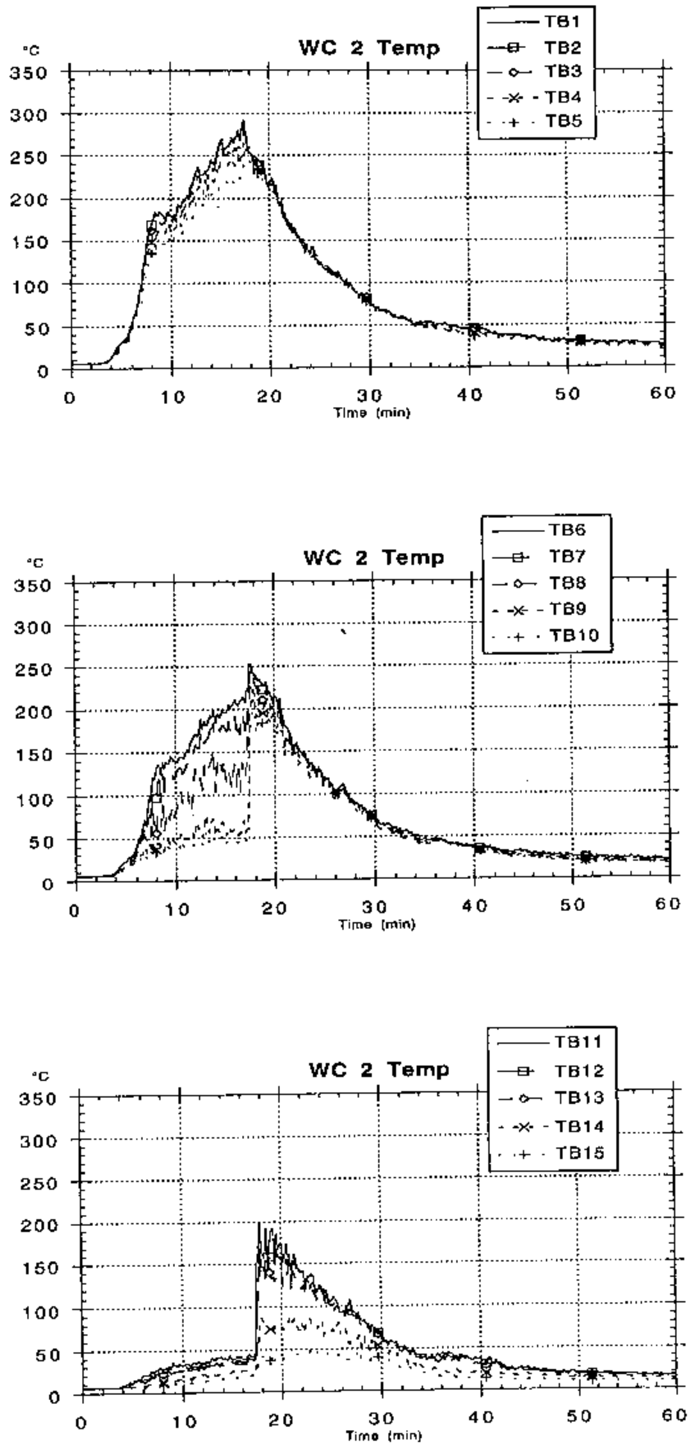

Figure 2. Temperature at instrument-station B.

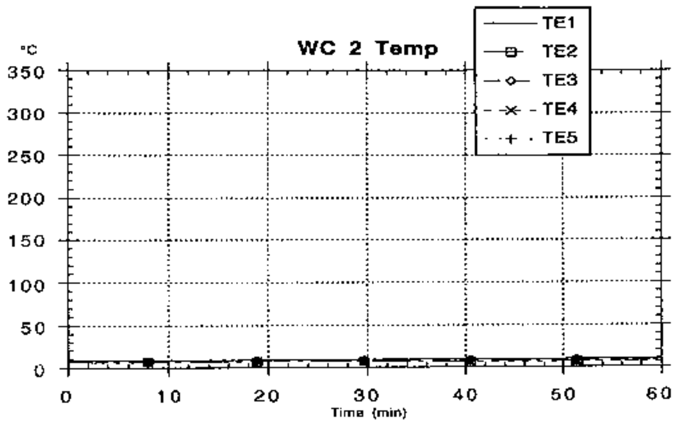

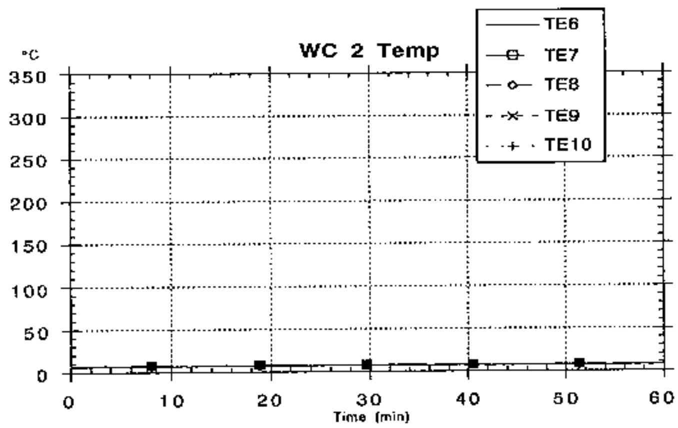

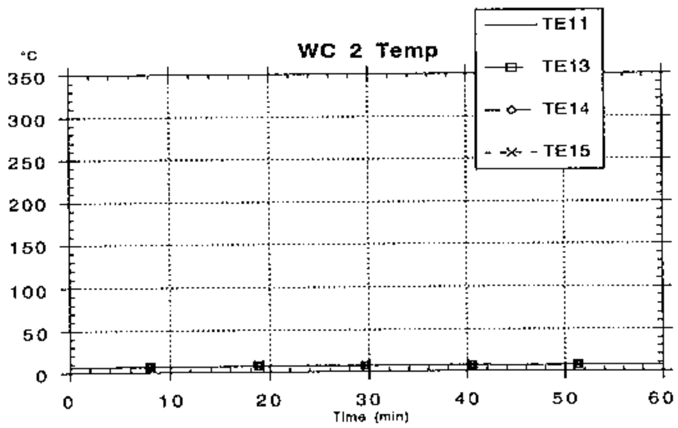

Figure 3. Temperature at instrument-station E.

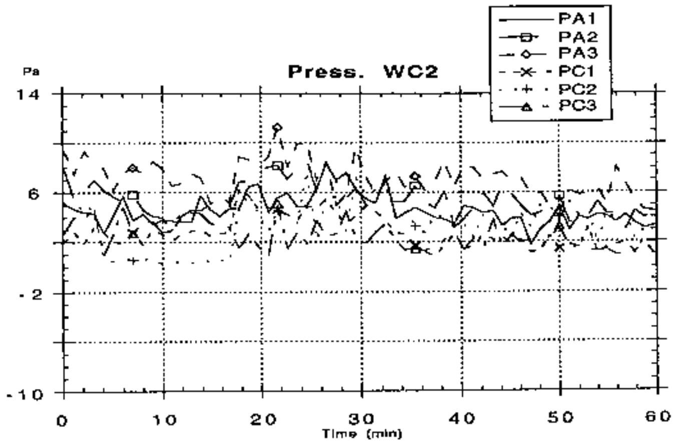

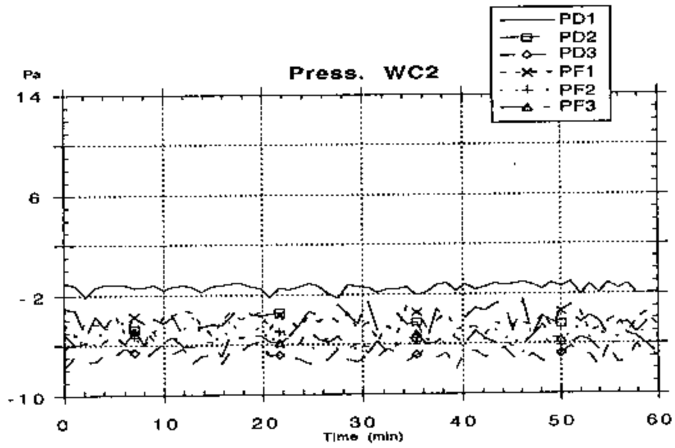

Figure 4. Pressure at instrument-station A, C, D and F.

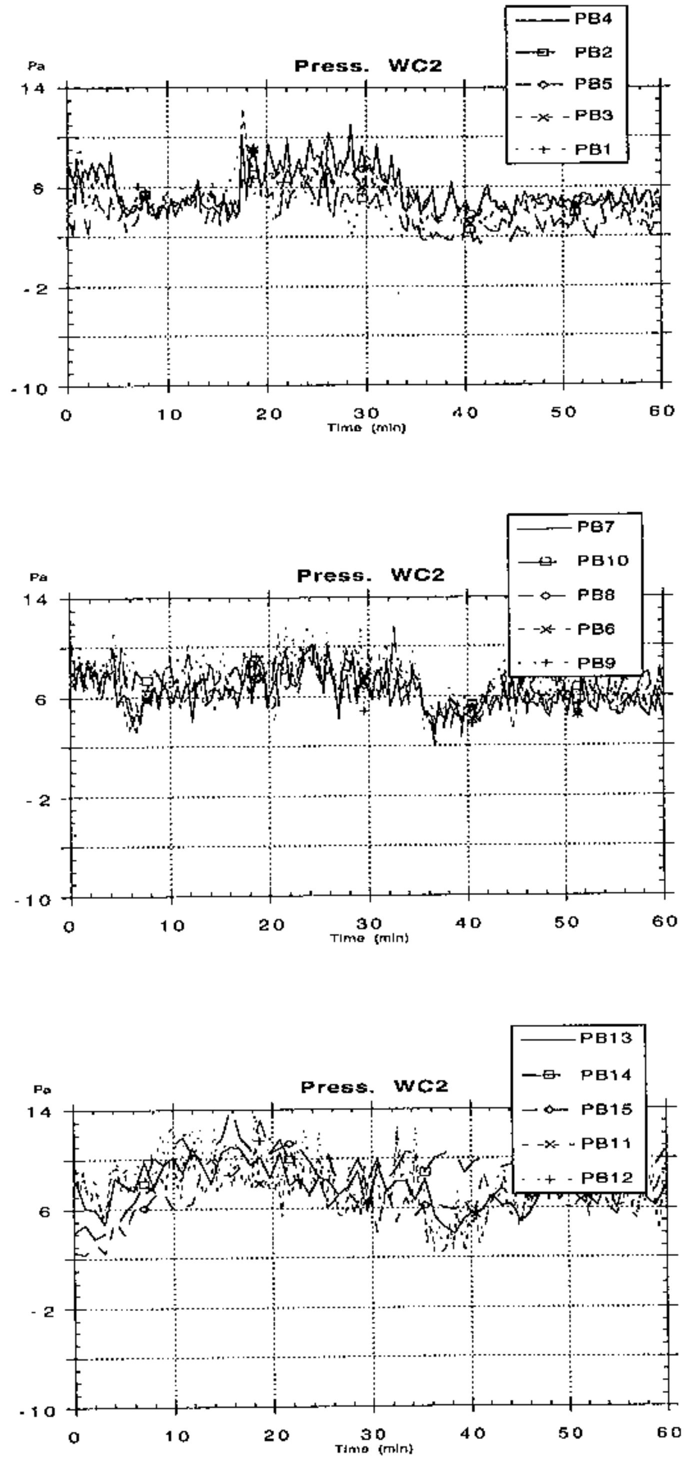

Figure 5. Pressure at instrument-station B.

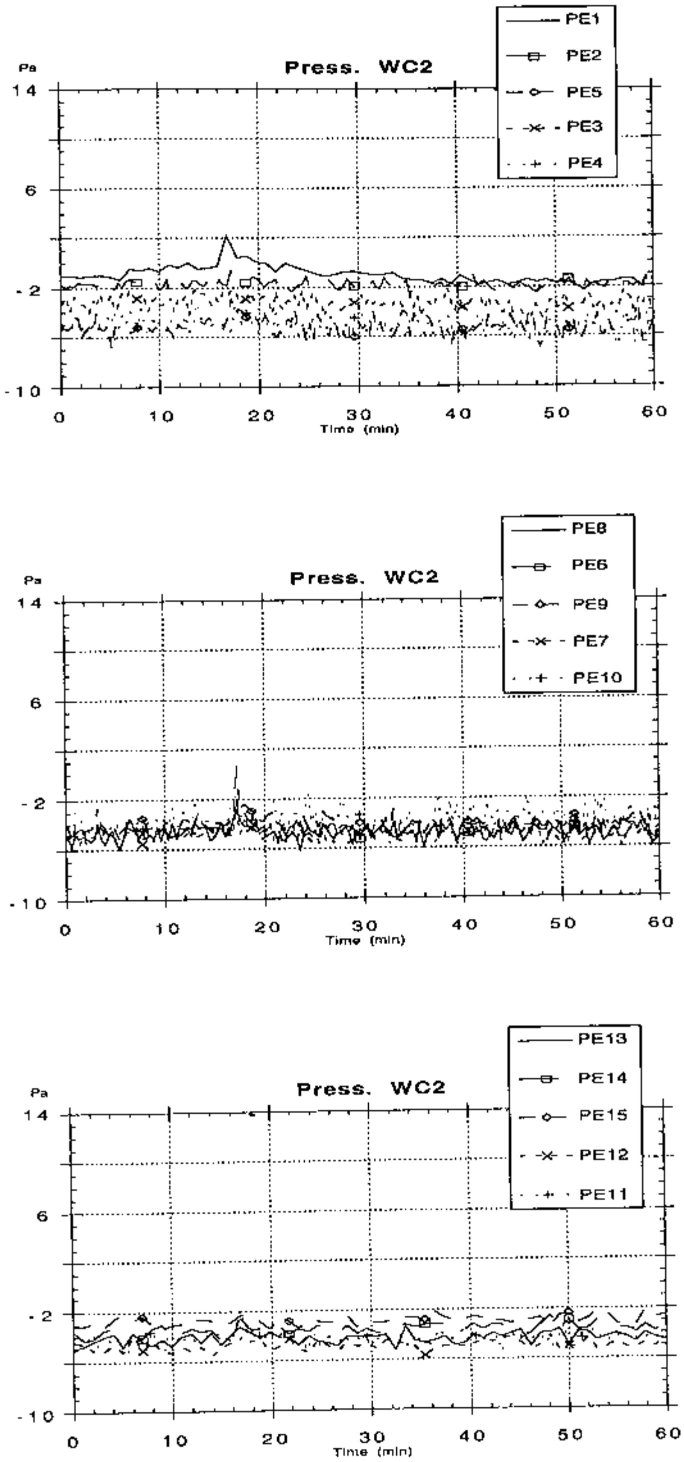

Figure 6. Pressure at instrument-station E.

Appendix D

Test results: railway wagon (F11)

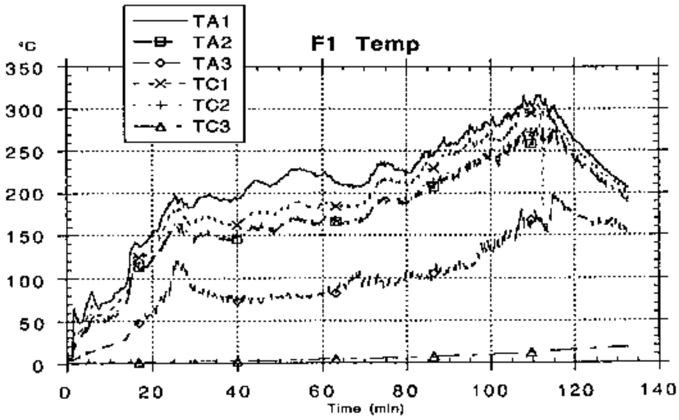

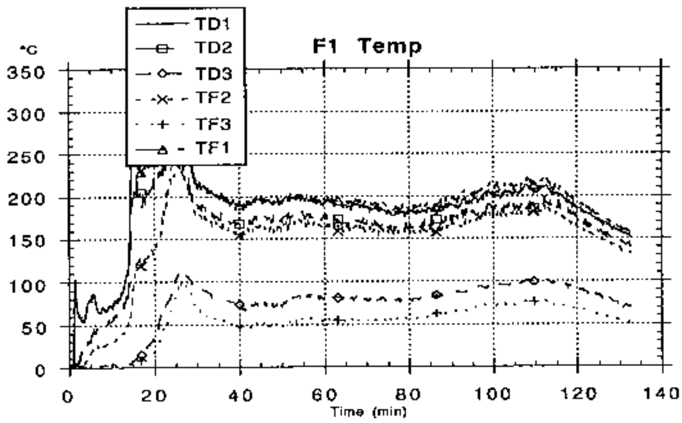

Figure 1. Temperature at instrument-station A, C, D and F.

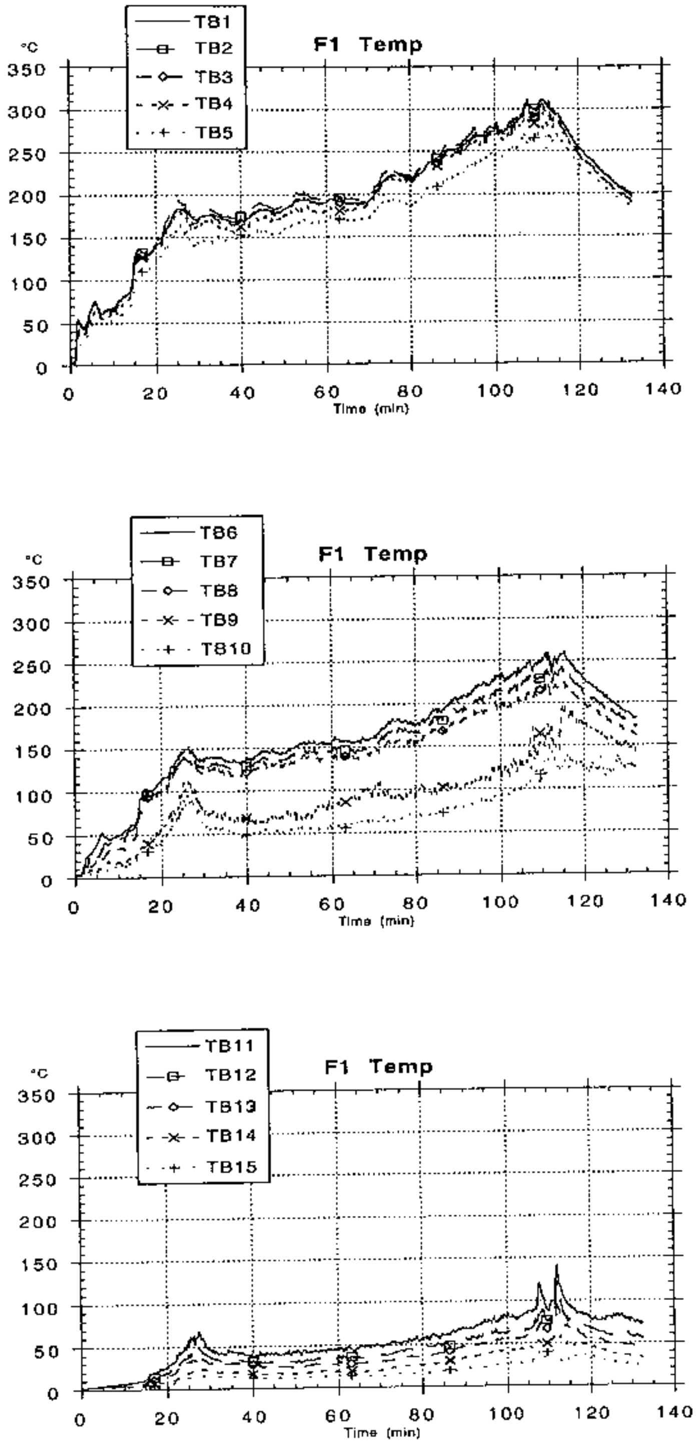

Figure 2. Temperature at instrument-station B.

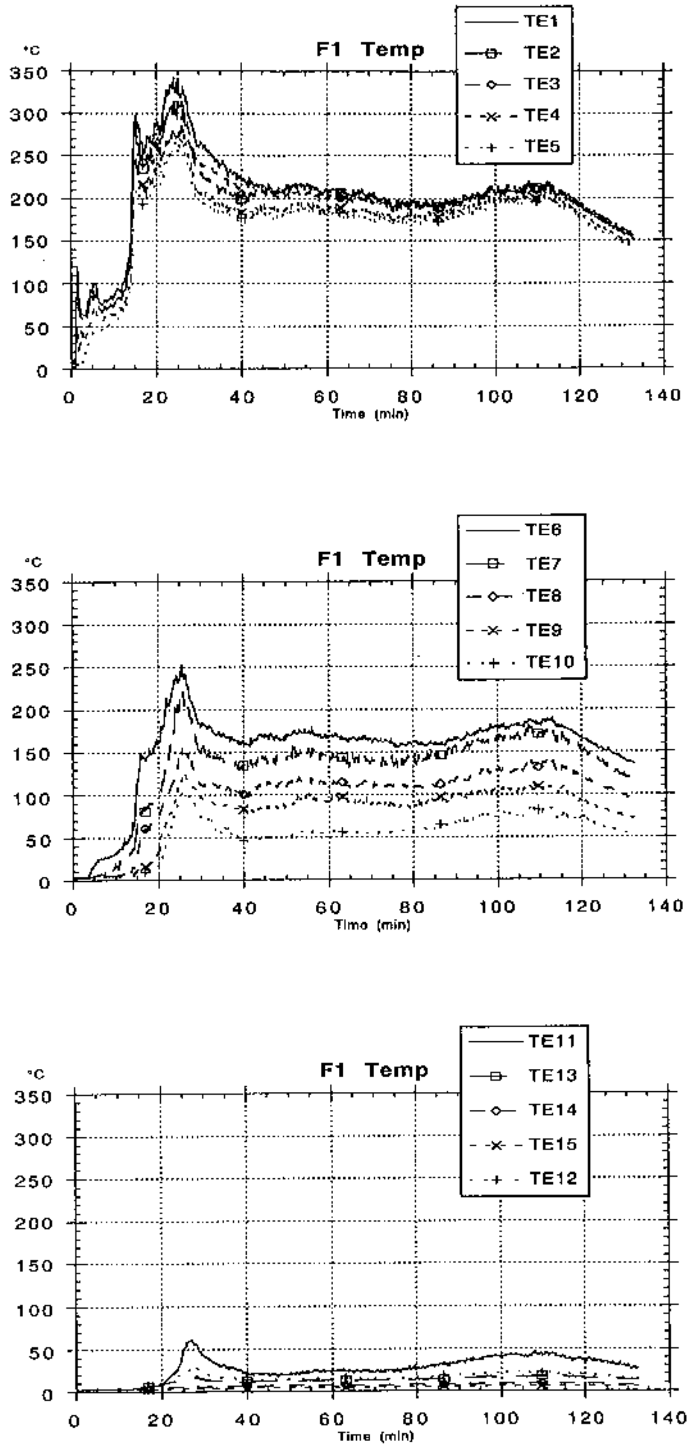

Figure 3. Temperature at instrument-station E.

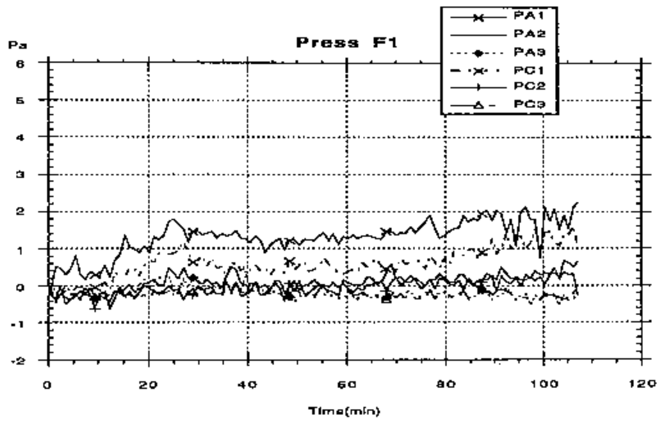

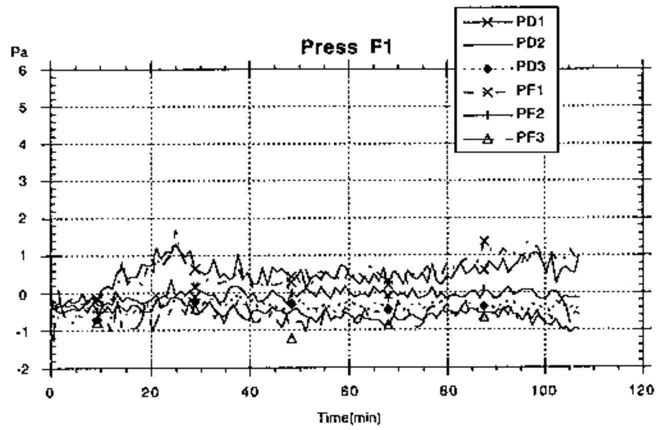

Figure 4. Pressure at instrument-station A, C, D and F.

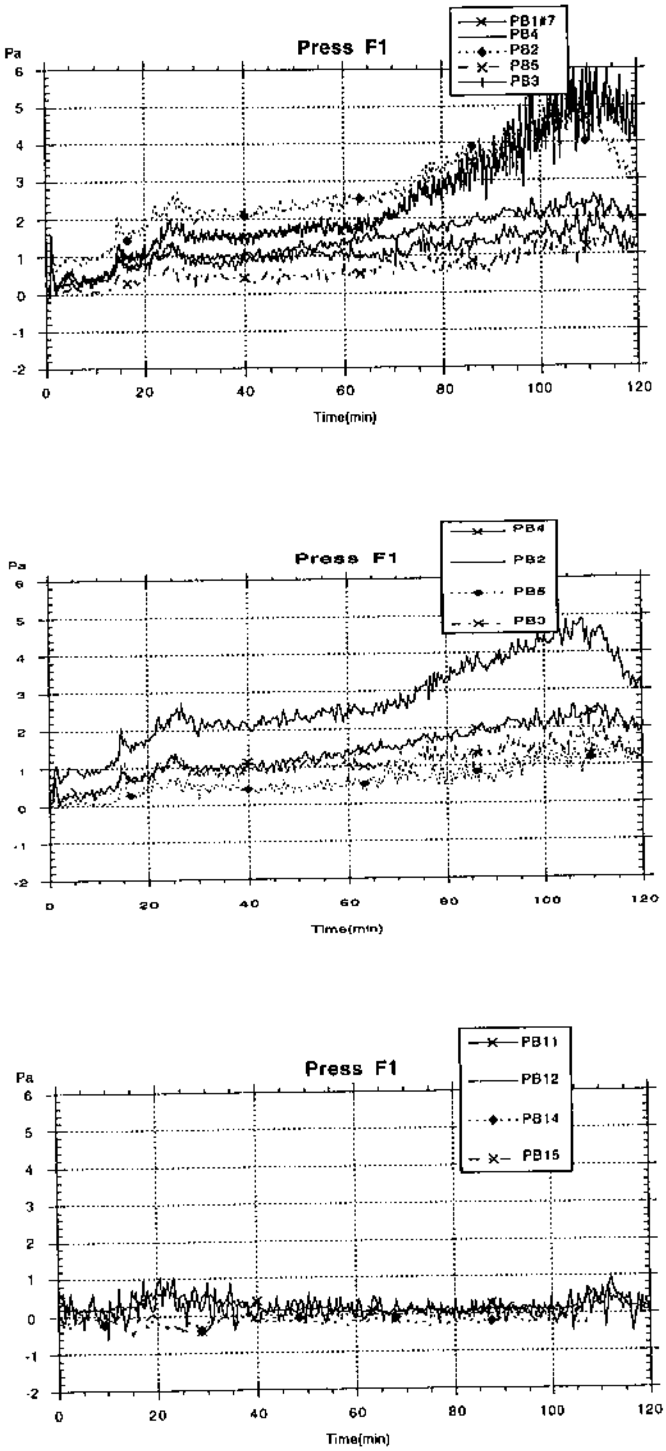

Figure 5. Pressure at instrument-station B.

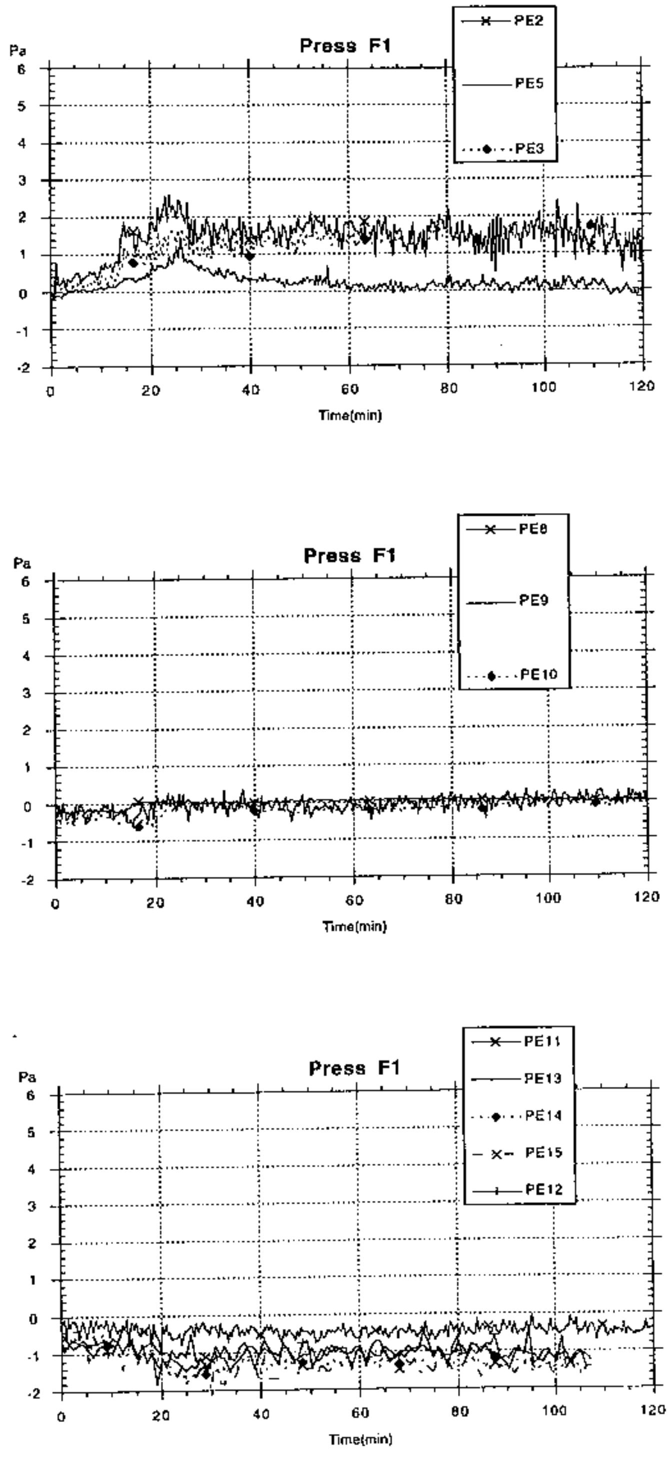

Figure 6. Pressure at instrument-station E.

Appendix E

Test results: subway train (F42)

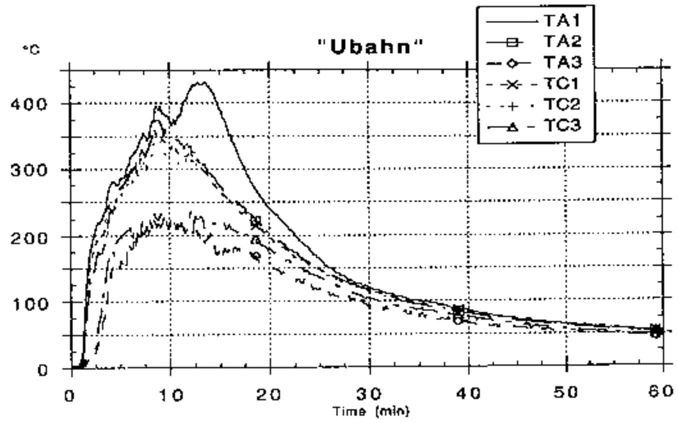

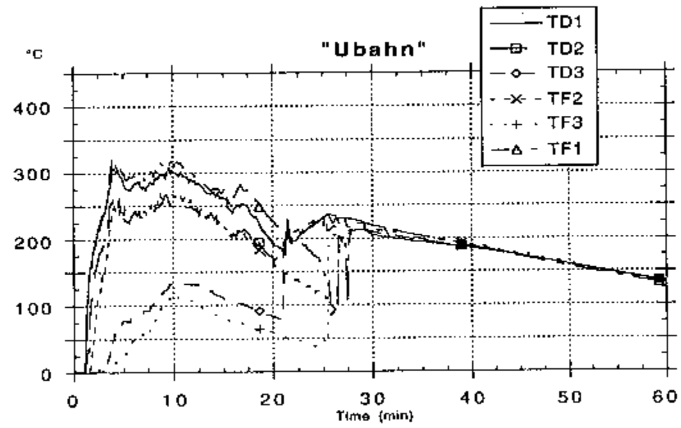

Figure 1. *Temperature at instrument-station A, C, D and F. The comparsation-cable was burnt off at appr. 25 min.*

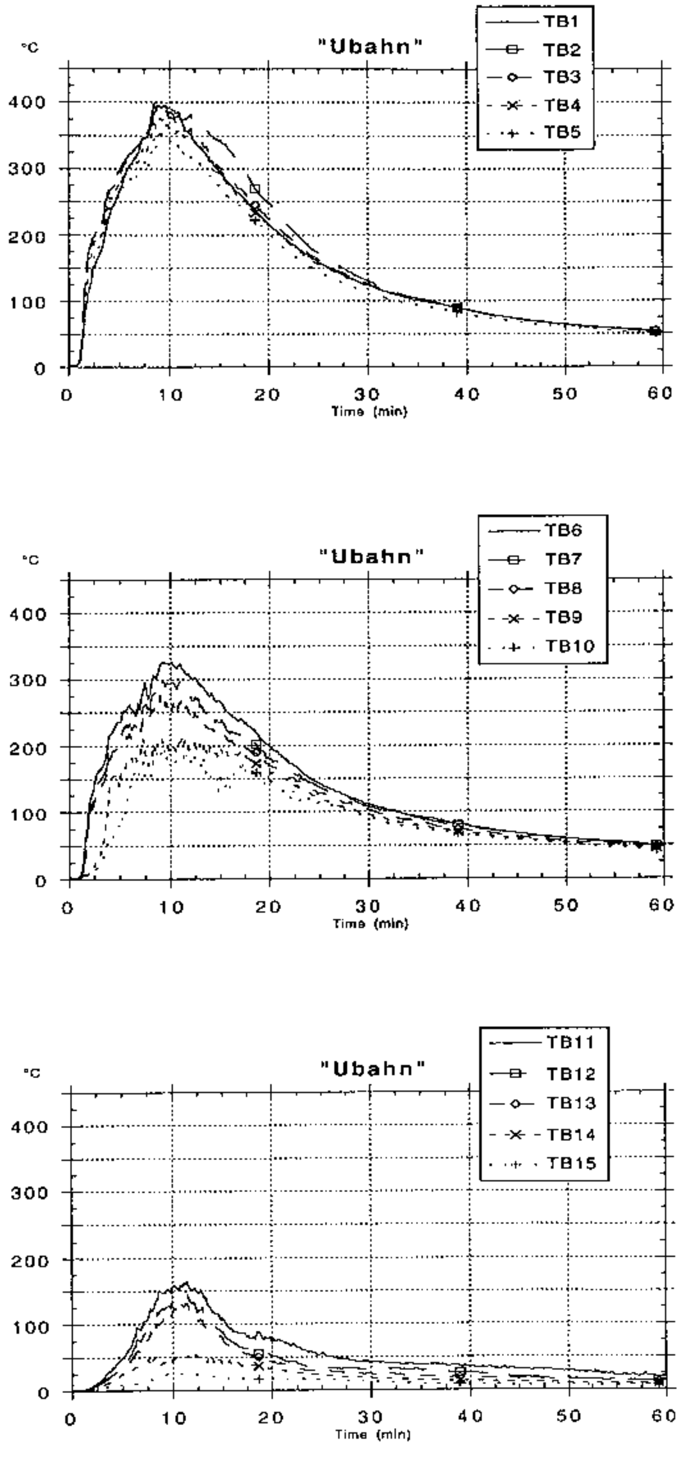

Figure 2. Temperature at instrument-station B.

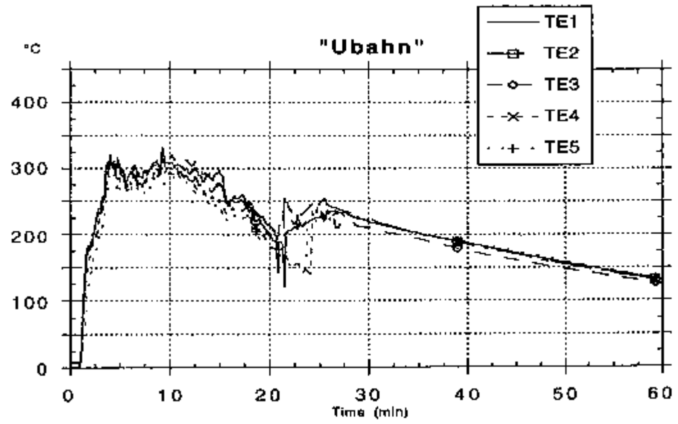

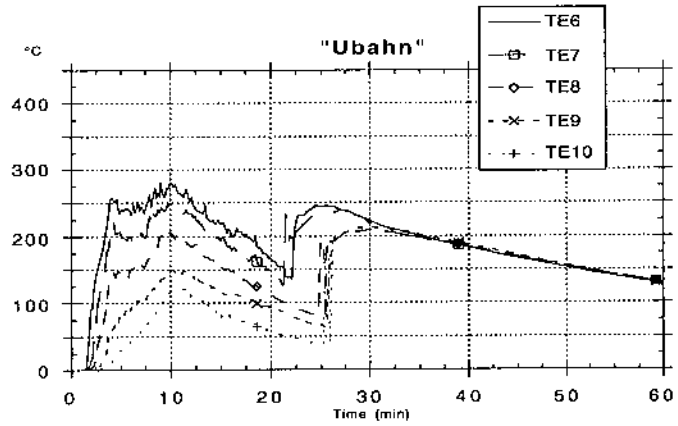

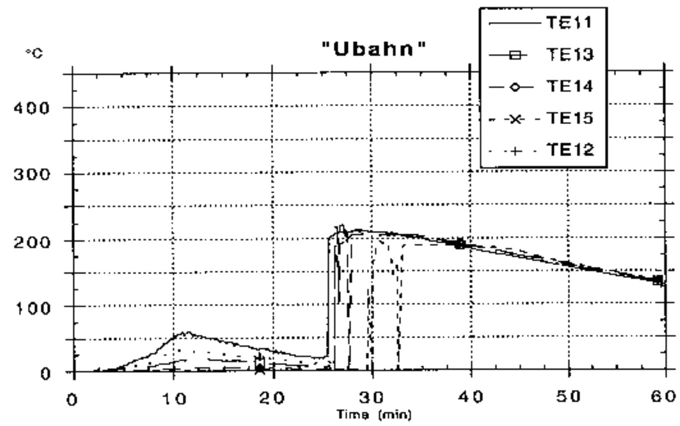

Figure 3. Temperature at instrument-station E. The comparsation-cable was burnt off at appr. 25 min.

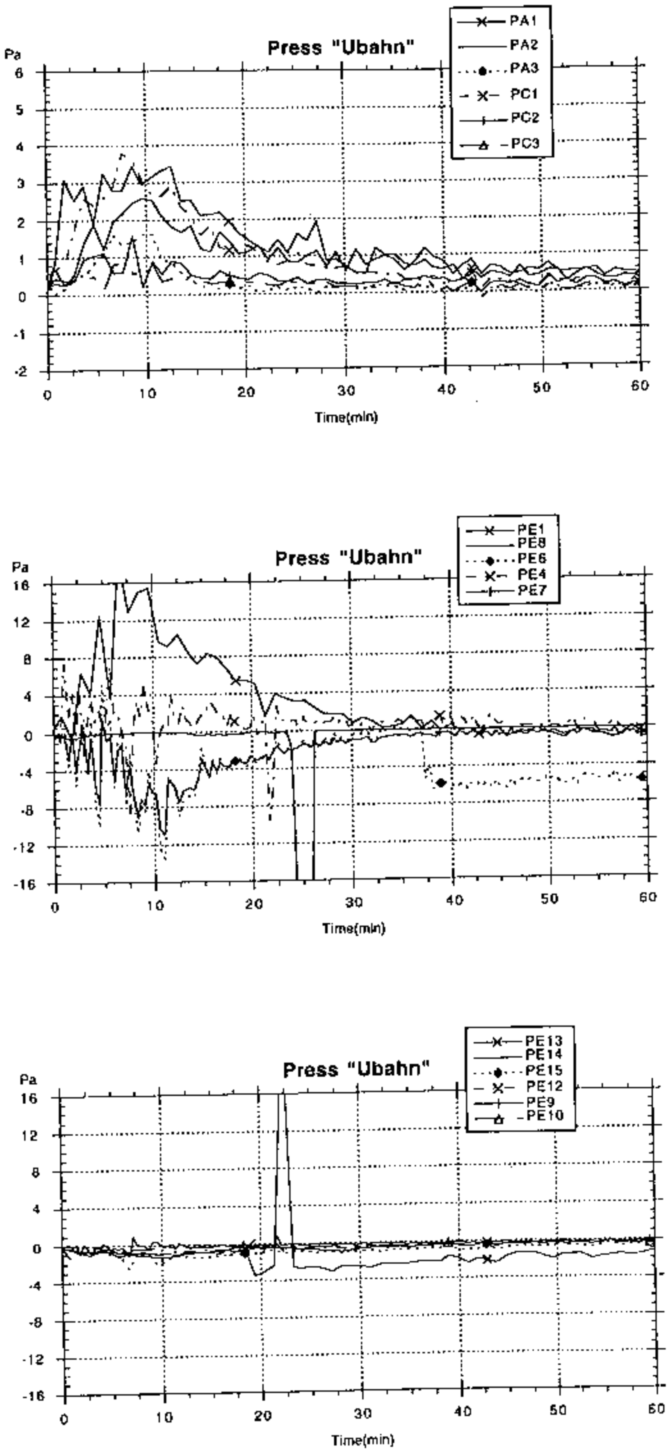

Figure 4. *Pressure at instrument-station A, C and E. The tubes for pressure-messurements were burnt off at appr. 25 min.*

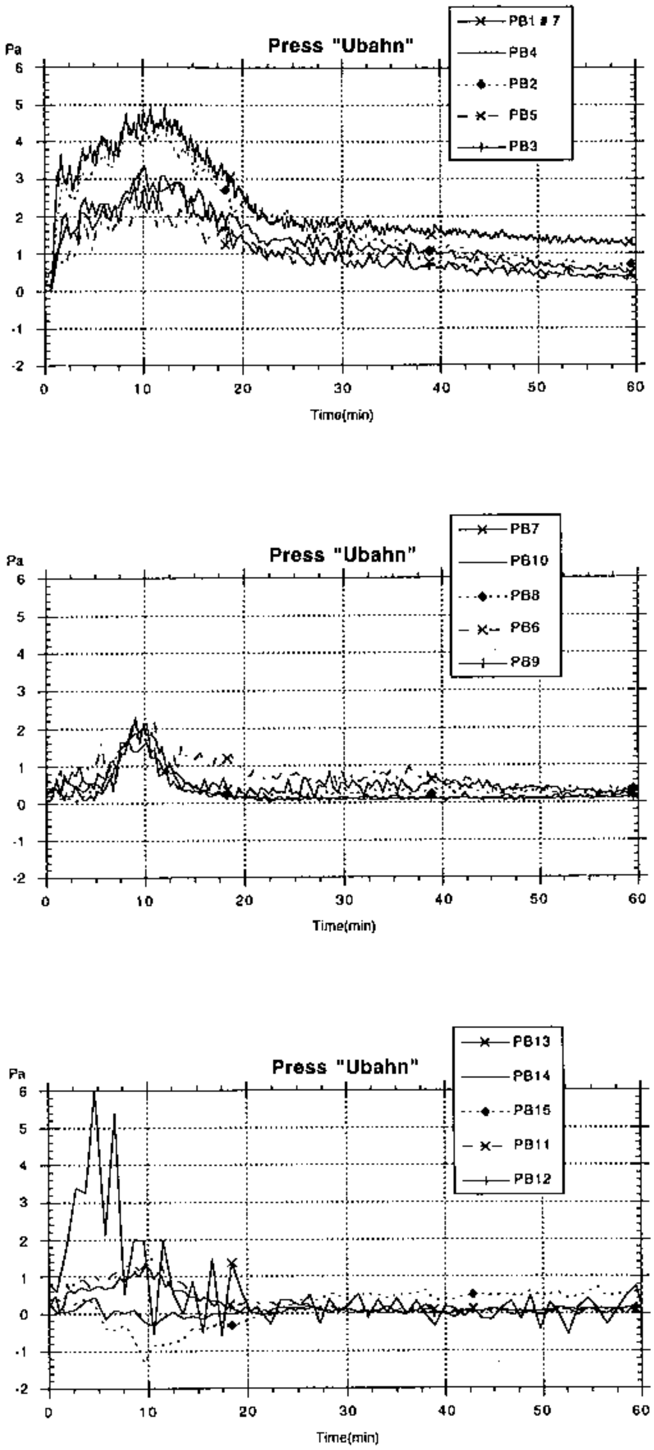

Figure 5. Pressure at instrument-station E.

Appendix F

Test results: simulated truck load (LF1)

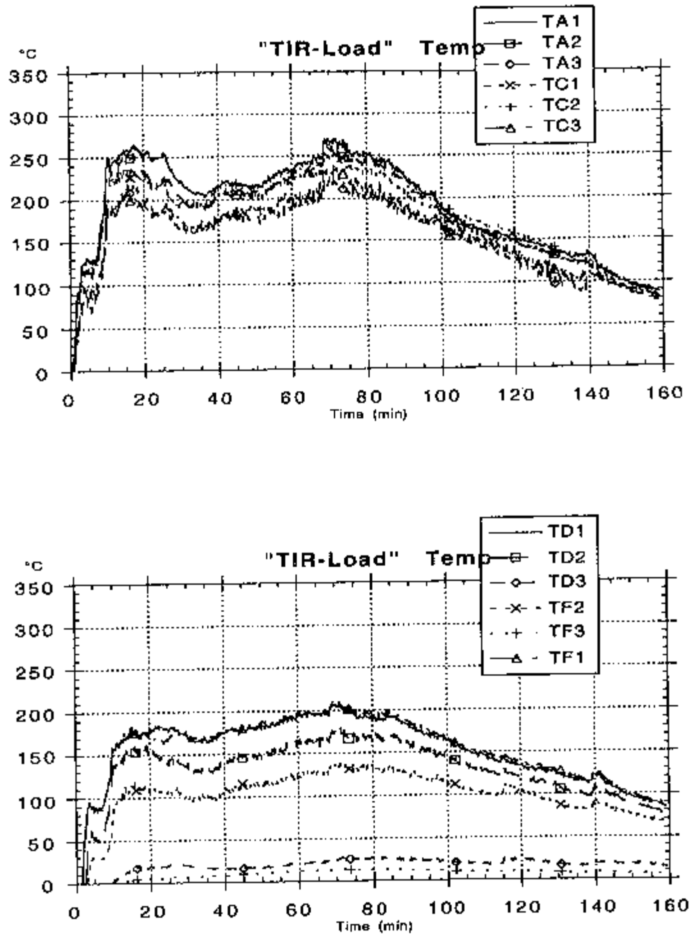

Figure 1. Temperature at instrument-station A, C, D and F.

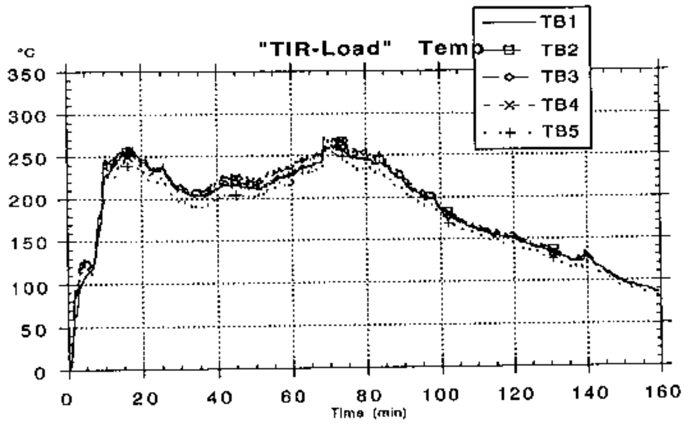

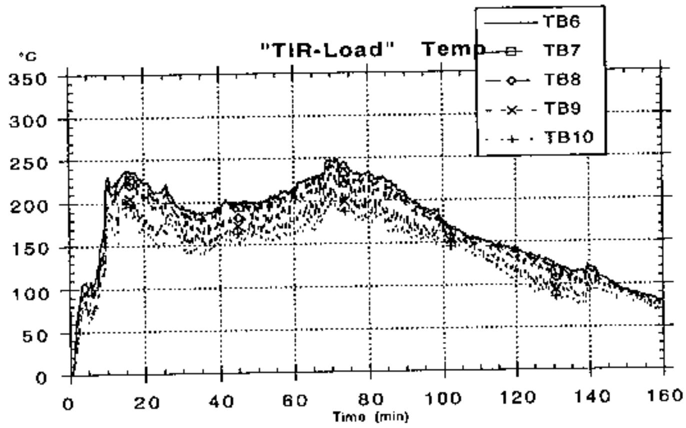

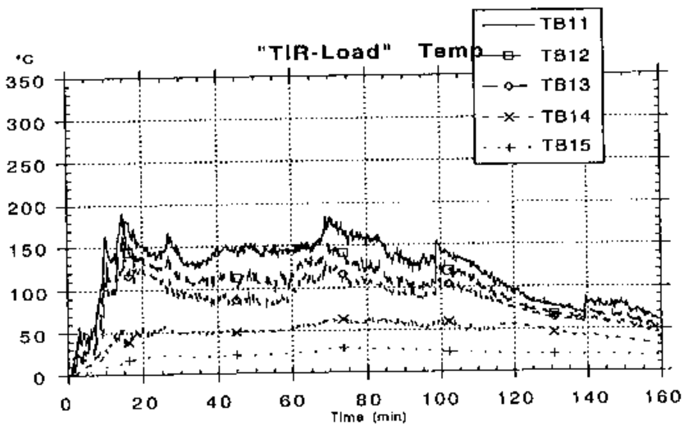

Figure 2. Temperature at instrument-station B.

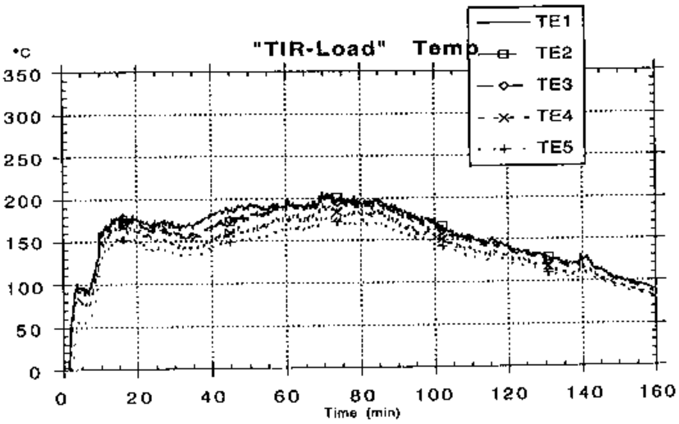

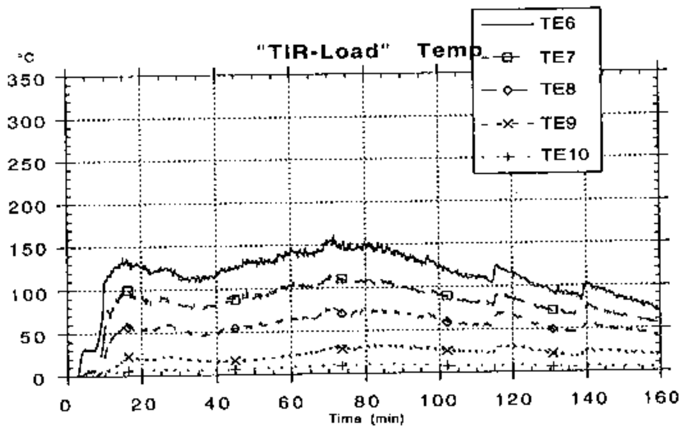

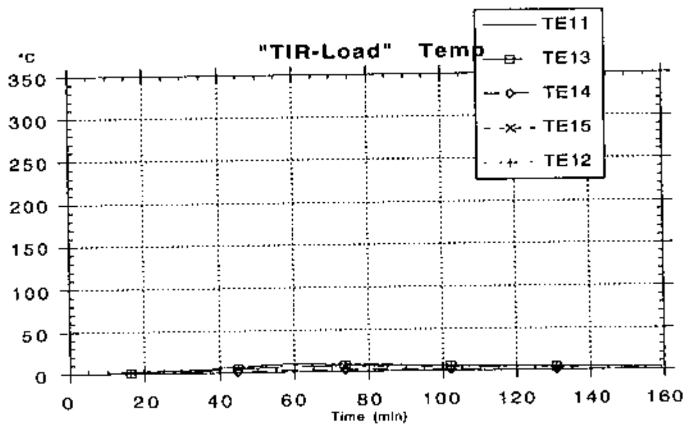

Figure 3. Temperature at instrument-station E.

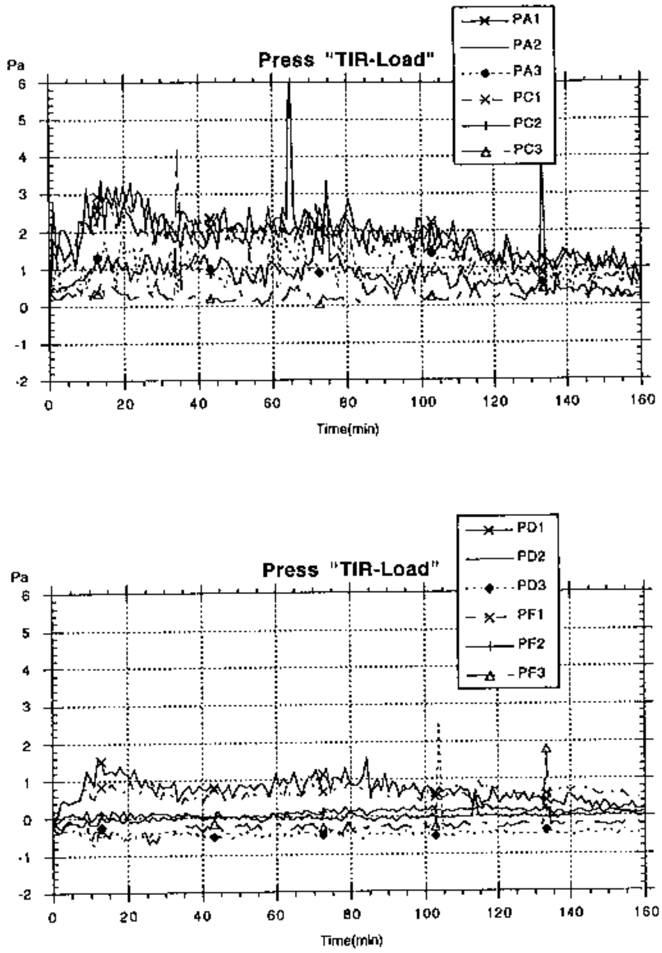

Figure 4. Pressure at instrument-station A, C, D and F.

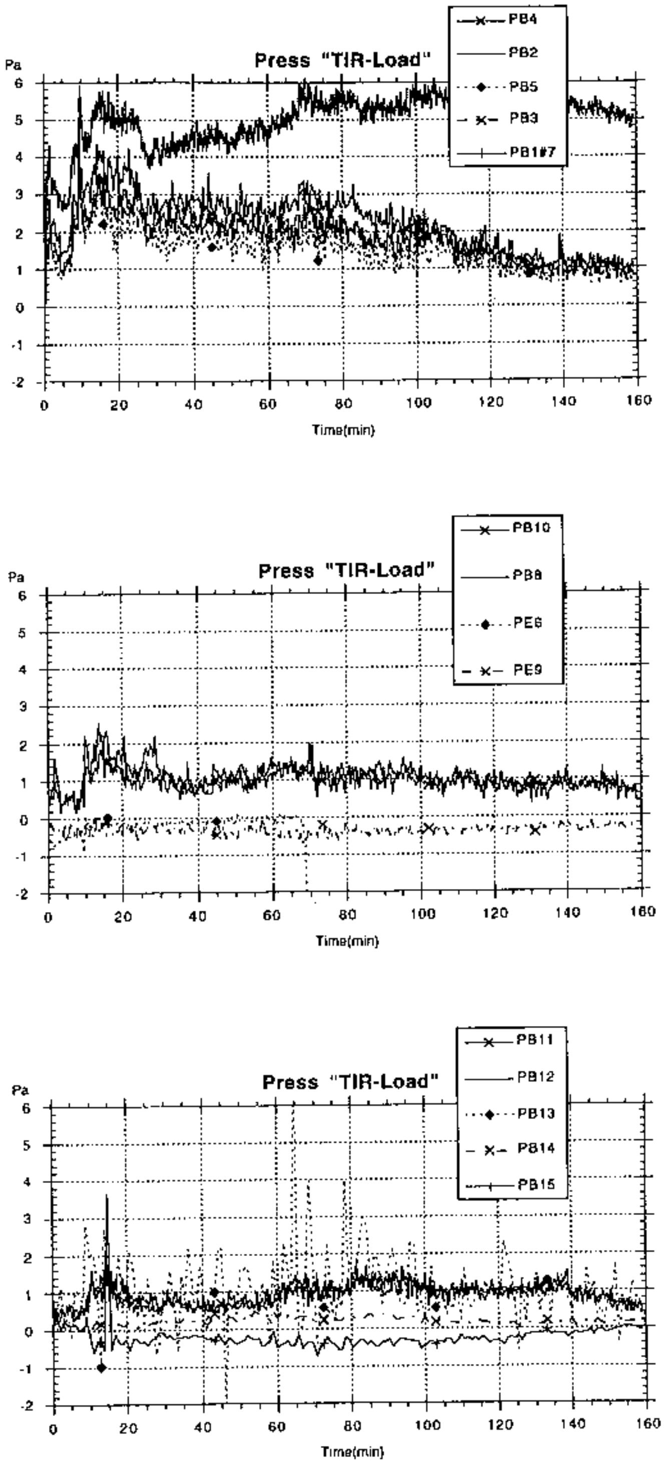

Figure 5. Pressure at instrument-station B.

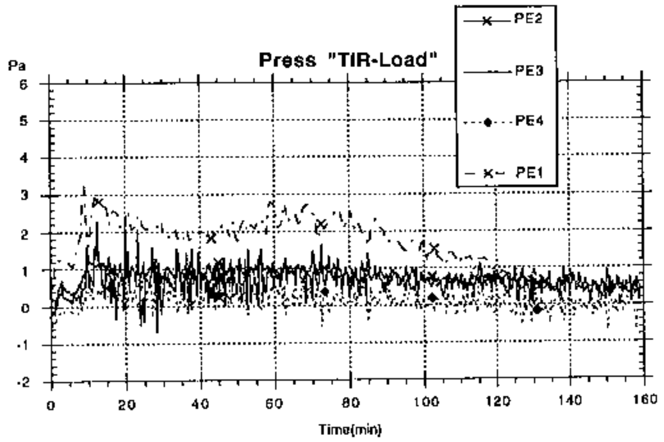

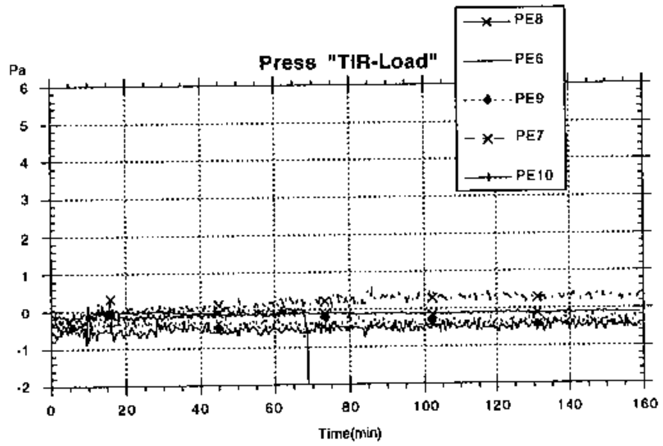

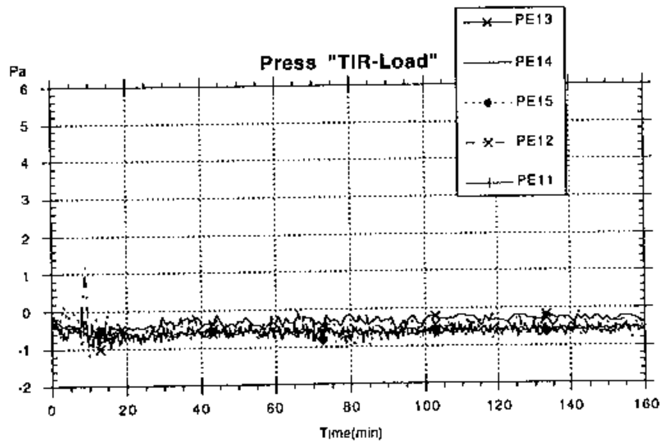

Figure 6. Pressure at instrument-station E.

Appendix G

1 Convective Heat Release Rate

In the following figures, calculated convective heat release rates from five tests are presented. Detailed information about the tested vehicles can be obtained from the technical report for the EUREKA 499 - project [1].

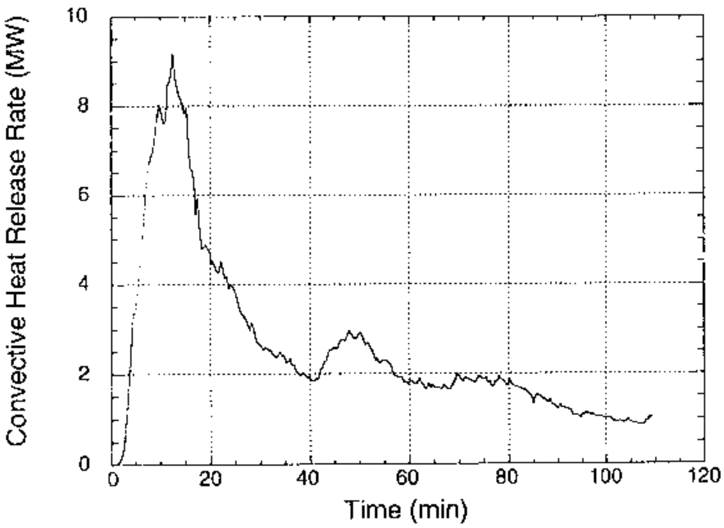

Figure 1 Convective heat release rate (HRR_{conv}) from a test with a schoolbus.

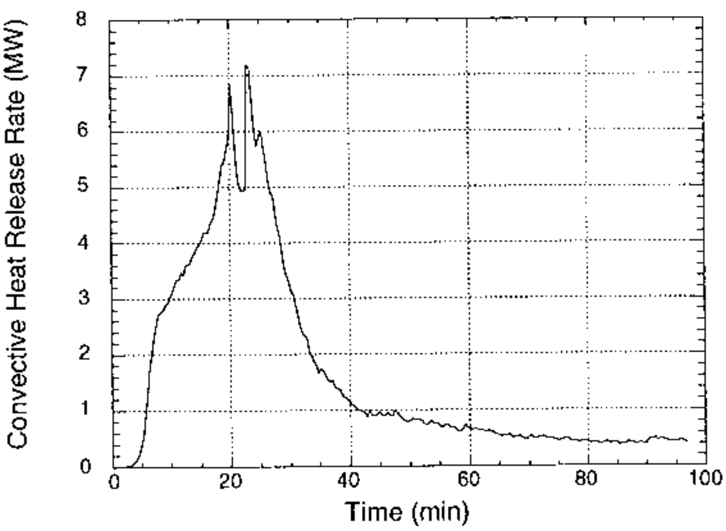

Figure 2 Convective heat release rate (HRR_{conv}) from a test with a wood crib without fans.

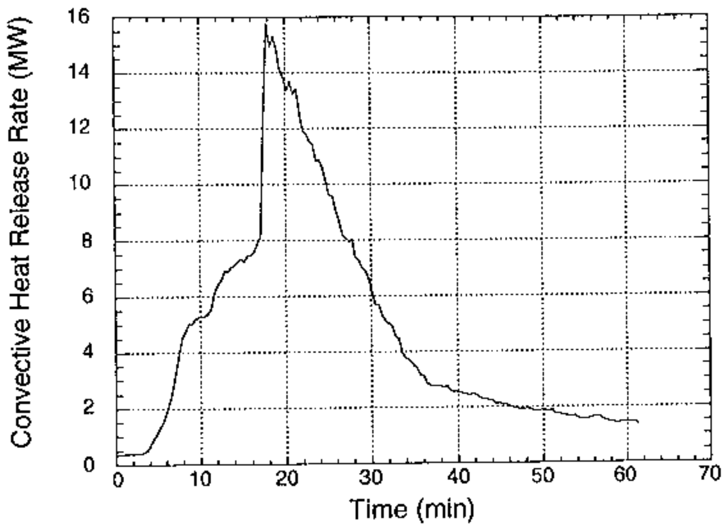

Figure 3 Convective heat release rate (HRR_{conv}) from a test with a wood crib with forced ventilation (velocity=2.9m/s).

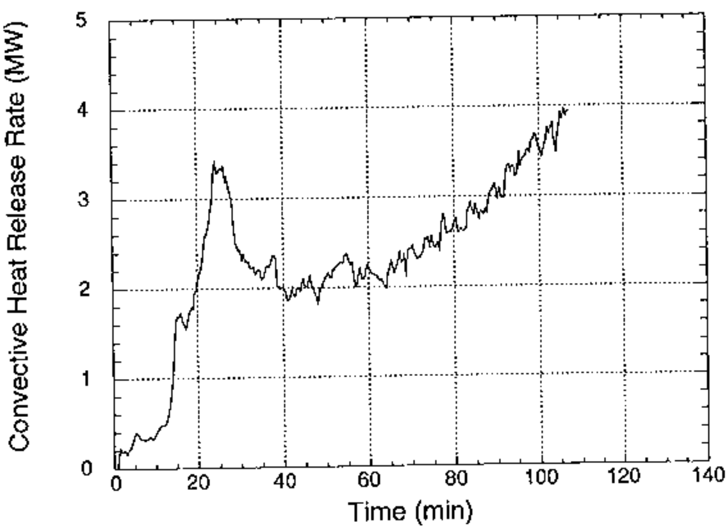

Figure 4 Convective heat release rate (HRR_{conv}) from a test with a passenger train.

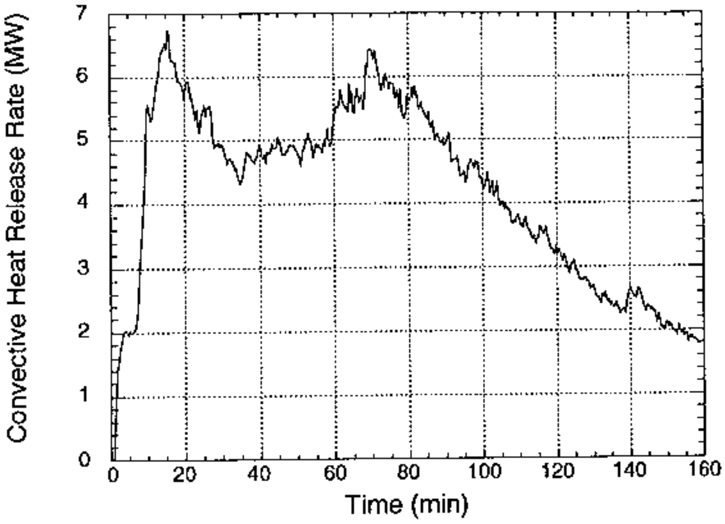

Figure 5 Convective heat release rate (HRR_{conv}) from a test with a simulated truck load.

Appendix H

Error analysis

In the following a conservative estimation of the error for instruments and calculation procedureis is given. The errors are conservatively added (maximum error).

Mass flow rate

Table 1 Uncertainty in massflow

Error limits	Explanation
±6 %	Variation in the choice of area division and missing measuring points
±2 %	Instrumental errors (temperature and pressure)
SUM: ±8 %	

HRR

Table 2 Uncertainty in HRR

Uncertainty	Explanation
mass flow	See Table 1
±5 %	Low number of measurement points for the oxygen measurements, subjective estimation
< 1 %	Air humidity
±1 %	Instrumental errors (oxygen concentration)
±5 %	Heat of combustion value E
±5 %	Combustion process
SUM: ±25 %	

HRR_{conv}

Table 3 Uncertainty in HRR_{conv}

Uncertainty	Explanation
mass flow	See Table 1
SUM: ±8 %	

SP
Swedish National Testing and Research Institute
Box 857, S-501 15 BORÅS, Sweden
Telephone: +46 33-16 50 00, Telefax: +46 33-13 55 02

SP REPORT 1994:08
ISBN 91-7848-XXX-X
ISSN 0284-5172